Construction and Building Materials 427 (2024) 136213

Contents lists available at ScienceDirect

Construction and Building Materials

journal homepage: www.elsevier.com/locate/conbuildmat

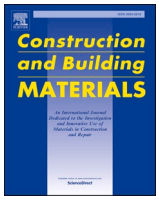

Durability of bond between EBR-CFRP laminate and concrete after four years of natural outdoor and accelerated ageing exposures

Aloys Dushimimana [a], José Sena-Cruz [a,*], Luís Correia [a], João Miguel Pereira [a], Susana Cabral-Fonseca [b], Ricardo Cruz [a]

[a] University of Minho, ISISE/IB-S, Department of Civil Engineering, Guimarães, Portugal
[b] National Laboratory for Civil Engineering, Materials Department, Lisbon, Portugal

ARTICLE INFO

Keywords:
Bond
Concrete
Epoxy adhesive
CFRP
Ageing
Moisture
Freeze-thaw
Temperature
Carbonation
Airborne chlorides

ABSTRACT

Application of carbon fibre reinforced polymer (CFRP) composites in strengthening of existing reinforced concrete (RC) structures has been widely accepted. However, the durability of adhesively bonded CFRP-concrete joint has not yet been fully investigated, which therefore paves the way to the topic addressed in this work: the durability of the joint in concrete elements strengthened with CFRP laminate using externally bonded reinforcement (EBR) technique. Concrete strengthened elements were kept in laboratory-controlled environments (approximately 20 °C/55 % RH, and water immersion at 20 °C), while others were kept outdoor to mainly promote natural ageing by carbonation, high temperatures, freeze-thaw attacks, and airborne chlorides. The results from durability tests after 4 years of exposure showed insignificant bond strength degradation but with a noticeable bond stiffness reduction, also, the stiffness degraded faster than the strength. Besides, environmental conversion factors of 0.75 and 0.95 were derived from a database of existing accelerated ageing test data and the natural ageing test data from the present work, respectively.

1. Introduction

A significant number of existing reinforced concrete (RC) structures around the globe are old, hence there is a growing demand for possible solutions that can be used to preserve and/or extend the service life of such structures. One of the possible solutions is the application of strengthening systems. The materials to be used should have desirable short-term and long-term performance properties to improve the overall performance of the structure, and also be environmentally friendly, possessing a high sustainability index. One of the best candidates for such materials is carbon fibre reinforced polymer (CFRP) composites, which possess a lower environmental impact than glass FRP (GFRP) [1] and other alternative materials, if produced using a recycling approach [2]. CFRP composites have been shown to possess excellent properties including high strength to weight ratio, high durability, and high corrosion resistance [3], among others. It is worth noting that CFRP composites are typically produced as either in situ cured sheets or pre-fabricated (precured) pultruded laminates. The former is generally used for shear strengthening due to its flexibility to deform into any desired shape, e.g. [4], while the latter is commonly used for flexural strengthening, e.g. [5]. In this work, CFRP laminates were adopted since this study is part of a research project where this type of FRP system was used to strengthen RC slabs with passive and pre-stressed active systems [35]. The CFRP laminates can be bonded to existing RC structures using an epoxy adhesive as a bonding agent, and the application can be through externally bonded reinforcement (EBR) or near-surface mounted (NSM) strengthening technique [6]. Focusing on the EBR-CFRP technique, the CFRP is typically bonded on the surface of the element to be strengthened [7]. In general, the durability of EBR-CFRP is still an open area of research, as there is a lack of knowledge on the long-term performance of CFRP-to-concrete bond and its constituent materials as well.

The durability of concrete when exposed to different degradation agents has been investigated. In fact, concrete carbonation depth can be affected by some agents, for example, low relative humidity (RH) and high temperatures can render concrete more porous, thereby allowing carbonation depth increase [8–10]. Contrary, low temperatures (below 9 °C) [11] and continuous cement hydration [12] will generally prevent CO_2 penetration. Besides, carbonation depth increases in environment with 50–70 % RH [8] and can increase optimally at 65 % RH [11].

* Corresponding author.
E-mail address: jsena@civil.uminho.pt (J. Sena-Cruz).

https://doi.org/10.1016/j.conbuildmat.2024.136213
Received 11 December 2023; Received in revised form 11 March 2024; Accepted 8 April 2024

Studies have shown that when concrete is exposed to carbonation [12] or to ultraviolet radiation (UV) with certain humidity and temperature [13], its compressive strength will increase. Both concrete compressive strength and elastic modulus increased after being exposed to carbonation [14]. Besides, carbonation reduced the effect of chlorides on the concrete surface by increasing the effect at the concrete inner region (>3 mm depth) as exposure time increased [15]. This was also found in other studies [16], where carbonation released the bound chlorides (from Fridels salt) inward at greater depth.

On the other hand, epoxy adhesive properties can also be affected by various degradation factors. In fact, studies show that exposure of epoxy adhesive to moisture and water can significantly deteriorate its properties [15,16]. Exposure to temperatures closer to the adhesive's glass transition temperature (T_g) can lead to deterioration of its properties [18] through softening of the polymeric matrix viscoelasticity; moreover, a synergy between moisture and temperature may lead to higher degradation effects [19]. However, elevated temperatures will positively lead to improved adhesive properties (e.g., higher strength and stiffness) thanks to post-curing phenomenon [20]; wet-dry cycles can reduce both the adhesive tensile strength and elastic modulus [21], while exposure to chlorides does not lead to detrimental effect [22]. Furthermore, a study by [23] reported that high carbonation can increase the curing of epoxy resin.

Regarding the durability of CFRP laminate, existing studies show that CFRP is immune against chloride exposure [18], and thermal cycles [24] although microcracking of the fibre matrix can develop as a result of different coefficient of thermal expansion (CTE) between the fibre and matrix [18]. Besides, freeze-thaw (FT) cycles can decrease both tensile strength and elongation of CFRP [25], moisture can affect the properties, particularly at fibre-matrix level [26], UV may also affect a few microns from the CFRP surface [26]. Additionally, in outdoor environment, UV is combined with effects of temperature, moisture, and FT, among others [18]. Hence, more studies are needed to be able to better understand the behaviour of CFRP laminate, particularly in outdoor exposure.

The durability of EBR CFRP-to-concrete bond has also been investigated using accelerated ageing test (AAT) protocols, e.g., [24,27–34]. According to these studies, 20 FT [30], 50, 150, and 300 FT [27], and 100 and 200 FT (for specimens with 400 mm bond length) [29] increased the bond strength; however, a reduction of bond strength was observed after 300FT [32] and 30, 60, 90 FT in [34]. Furthermore, water immersion for durations of 1000 and 3000 h at 22 and 38 °C [30], 2880 h [32] increased the bond strength, while immersion for 330–1340 h [33] and 10,000 h at 22 °C [30] decreased the strength. Additionally, elevated temperatures of 50 °C [28] increased the bond strength but 60 °C for 1000 h and 3000 h [30] decreased it; and thermal cycles between −18 and 30 °C for 2160 h in air increased the bond strength, while those in water decreased it [24]. Hygrothermal at 40 °C and 95 % RH for 4200 h increased the bond strength, whereas a decrease was observed using the same conditioning but for up to 8472 h [31]. Overall, a significant variability of the results from these studies is evident.

From the above literature, some knowledge gaps still exist: (i) most of existing studies were conducted under accelerated ageing test (AAT) protocols, while in reality strengthened structures are exposed to natural ageing; ii) there is a lack of studies under natural ageing test (NAT) protocols and the correlation between the AAT and NAT; (iii) environmental conversion factors (ECF) recommended in existing standards are based on studies solely performed under AAT; (iv) the recommended ECF ideally represents all degradation agents that are thought to promote ageing; however, in real applications, a structure is exposed to a combination of certain agents (not a single one nor all at once) depending on its location. In this regard, the main objective of this work was to try to address the above gaps by investigating the bond performance in concrete elements strengthened according to EBR-CFRP technique for the case when the bond is exposed to different accelerated (laboratory-controlled) and natural (carbonation, high temperatures, freeze-thaw attacks, and airborne chlorides) ageing environments. Besides, the ECF for the bond strength from the existing AAT data were derived, and some comparative studies between the ECF from existing AAT data and NAT data from the present work were performed.

2. Experimental program

The experimental campaign focused on the assessment of the EBR CFRP-to-concrete bond durability over time. In addition, specimens of the bond constituent materials (concrete, epoxy adhesive, and CFRP laminate) were also tested in order to have an advanced understanding of their effects on the bond behaviour.

2.1. Properties of the tested specimens

The properties of concrete, epoxy adhesive, and CFRP laminate are first described, followed by those of the EBR CFRP-to-concrete bond.

Concrete: the concrete used to prepare all specimens for determining the concrete compressive strength (f_{cc}), elastic modulus (E_c), pull-off strength (f_{ct}), and carbonation depth (C_d), was cast using the same batch as that of the single lap shear tests specimens. The concrete properties were as shown in Table 1. Concrete cylinders (Fig. 1a) were produced to determine the E_c and f_{cc} properties. Concrete prisms (Fig. 1b) were used to assess the f_{ct}, C_d, as well as bond strength.

Epoxy adhesive: a two-component commercial cold-curing epoxy

Table 1
Materials and EBR CFRP-to-concrete bond properties.

Concrete		**Epoxy adhesive**	
Specimen type	Cylinder with D×H:150×300 [mm^2]	Type of adhesive	Cold-curing S&P Resin 220
Max aggregate size [mm]	12.5	Flexural elastic modulus [GPa]	>7.1
Cement type	CEM II/A–L 42.5 R	Tensile strength [MPa]	19.9 (after 7d of curing at 20°C)
Slump [mm]	160–210 (slump class S4)	Glass transition temperature (T_g) [°C]	46.2 (after 7d of curing at 23°C)
Concrete class	30/37 MPa (C30/37)	Density, at 23 °C [g/cm^3]	1.7–1.8
Water-to-cement ratio	0.4	Compressive strength [MPa]	>70
f_{cc} [MPa], E_c [GPa]	41.5, 29.1 (after 28 days)	Shear strength [MPa]	>26
Exposure class	XC4(P)	BS by pull-off, on concrete [MPa]	3 (after 3d of curing at 20°C)
CFRP laminate		**EBR CFRP-to-concrete Bond**	
Type and trademark	S&P clever (CFK 150/2000)	CFRP cross-section [mm^2]	50×1.2
Prefabricated by	Pultrusion	Concrete prism dimensions [mm^3]	400×200×200
Fibre orientation	Unidirectional	Bond length [mm]	220
Fibre content [%]	68	Effective bond length [mm]	101
Fibre matrix	Vinyl ester resin (with $T_g \approx 85$°C)	Number of laminates per specimen	2
External surface	Black, smooth	Epoxy adhesive thickness [mm]	1.5–2.0
Elastic modulus [GPa]	>170	Type of test	Single-lap shear test
Tensile strength [MPa]	>2000		

f_{cc}: compressive strength (average value), E_c: elastic modulus (average value), BS: bond strength, D: diameter, H: height, T_g: glass transition temperature, d: days.

Fig. 1. Materials specimens used: (a) concrete cylinder, (b) concrete prism, (c) epoxy adhesive dog-bone shaped specimens and (d) CFRP laminates.

resin-based adhesive with properties shown in Table 1 was used to cast dog-bone shaped specimens (Fig. 1c) for determining the adhesive tensile strength (f_a) and elastic modulus (E_a). This adhesive is a solvent free, thixotropic, in grey colour, developed for bonding CFRP laminate to concrete.

CFRP laminate: the CFRP laminate (Fig. 1d) with properties as shown in Table 1 was used to assess its tensile strength (f_f) and elastic modulus (E_f) over time, and as a bond constituent material for strengthening purpose.

EBR CFRP-to-concrete bond: The EBR CFRP-to-concrete bond had properties as in Table 1.

2.2. Description of experimental stations

Six different environmental exposures (E1-E6) were used to promote degradation of both the EBR CFRP-to-concrete bond and its constituent materials. Different tests were performed on the specimens at initial time (denoted as T0) and on the specimens collected from the aforementioned environments after 1 year (T1), 2 years (T2), 3 years (T3) and 4 years (T4) of exposure. A description of the conditioning in each environment is provided as follows.

2.2.1. Laboratory accelerated conditioning

Two laboratory-controlled environments were considered. The first environment (denoted as E1) had the specimens conditioned at 20 °C /55% RH. The second environment (E2), see Fig. 2a, contained the specimens fully and continuously immersed in tap water at 20 °C. More detailed information can be found in [35].

2.2.2. Real-time field conditioning

Four different outdoor environmental exposures were selected with the aim to mainly promote degradation of the EBR CFRP-to-concrete bond and its constituent materials. The first outdoor environment (denoted as E3) was selected to promote the ingress of atmospheric carbon dioxide (CO_2) through the bond constituent materials, also known as *carbonation*. The second environment (E4) was selected to mainly promote the freeze-thaw attacks. The third environment (E5), see Fig. 2b, was selected to mainly promote degradation due to outdoor high temperatures. The fourth outdoor environment (E6) was selected to mainly promote the ingress of airborne chlorides (though the bond constituent materials) from the Atlantic Ocean, and high levels of humidity. It is worth noting that despite the target of conditioning the specimens with a single degradation agent, it is inevitable for the specimens in outdoor environments to experience more than one degradation agent. Hence there was a combination of degradation agents in each outdoor environment, e.g., in E3, there was both carbonation and elevated temperatures as dominant degradation agents, while in E4 both freeze-thaws and moisture were dominant.

The yearly recorded temperature and relative humidity (RH) are shown in Table 2, for all studied environments. It can be noted that the average of the yearly maximum temperatures in both E3 and E5 were the highest when compared to other outdoor environments. For example, in the first year (T1), the averages of the yearly maximum temperatures were 23.1 °C and 24.0 °C, and the yearly peak maximum values reached 46.2 °C and 44.6 °C, in E3 and E5, respectively. Furthermore, the RH in E6 was the highest for outdoor environments, followed by E3 and E4, respectively; hence confirming the significance effect of both

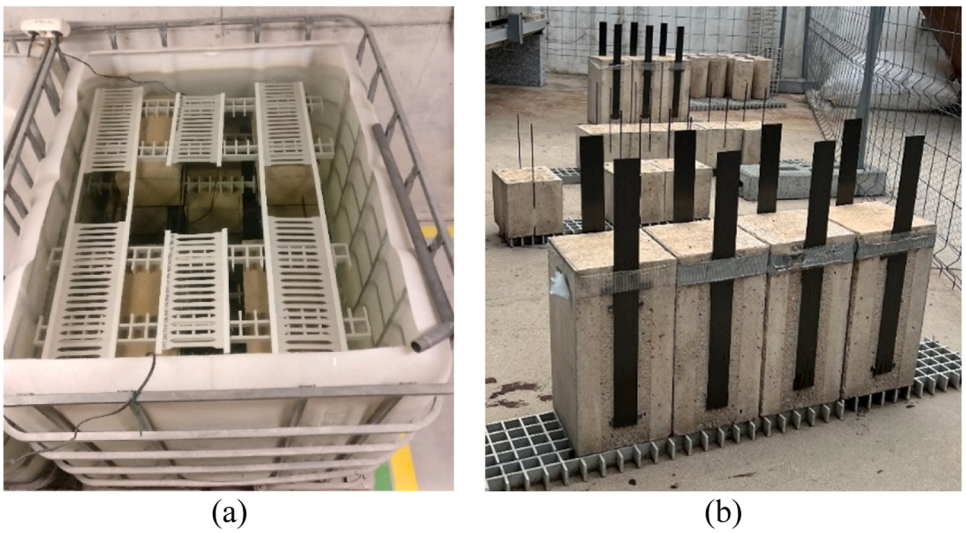

Fig. 2. Examples of environments considered: (a) laboratory-controlled (E2), and (b) outdoor conditioning (E5).

Table 2
Variation of yearly temperatures and relative humidity in the studied environments.

Variable / Environment		E1	E2	E3	E4	E5	E6
Temp [°C] Year 1 (T1)	Max	20.2 (22.5)	20.2 (20.3)	23.1 (46.2)	17.8 (32.4)	24.0 (44.6)	21.6 (36.0)
	Min	19.8 (13.5)	20.1 (19.0)	13.4 (3.3)	11.1 (-4.7)	11.1 (-1.9)	11.8 (1.5)
	Avg	19.9	20.0	17.4	14.3	17.4	16.15
RH [%] Year 1 (T1)	Max	62.8 (79.5)	100.0	87.9 (100.0)	83.3 (100.0)	84.9 (100.0)	88.7 (100.0)
	Min	57.8 (31.0)	100.0	48.8 (11.0)	50.9 (4.0)	40.3 (9.0)	59.8 (18.0)
	Avg	60.0	100.0	70.7	67.2	63.5	76.1
Temp [°C] Year 2 (T2)	Max	20.4 (22.0)	20.2 (20.4)	22.7 (39.7)	14.0 (29.6)	23.6 (39.9)	22.5 (39.5)
	Min	20.1 (19.0)	20.5 (19.5)	13.9 (4.3)	7.4 (-4.6)	8.9 (0.3)	13.0 (2.0)
	Avg	20.2	20.6	17.5	10.6	17.3	17.2
RH [%] Year 2 (T2)	Max	63.1 (77.5)	100.0	90.1 (100.0)	87.6 (100.0)	87.9 (100.0)	90.5 (100.0)
	Min	60.1 (41.5)	100.0	52.9 (16.0)	54.7 (4.0)	42.0 (11.0)	63.5 (28.5)
	Avg	61.8	100.0	74.4	72.8	67.1	78.6
Temp [°C] Year 3(T3)	Max	20.1 (22.0)	21.0 (22.0)	22.8 (40.7)	13.2 (29.5)	22.8 (41.4)	16.9 (31.1)
	Min	19.8 (17.0)	20.2 (19.6)	13.5 (1.4)	4.0 (-6.4)	11.4 (-4.1)	9.1 (-1.1)
	Avg	19.9	20.3	17.3	9.7	17.1	13.0
RH [%] Year 3 (T3)	Max	63.9 (77.5)	100.0	87.9 (100.0)	86.0 (100.0)	86.2 (100.0)	93.0 (99.0)
	Min	61.7 (43.0)	100.0	48.8 (16.0)	50.5 (6.0)	45.6 (9.0)	61.5 (23.0)
	Avg	62.9	100.0	70.7	71.3	66.5	79.4
Temp [°C] Year 4 (T4)	Max	20.5 (23.0)	20.2 (20.3)	-	20.7 (31.1)	25.5 (46.0)	19.9 (34.0)
	Min	20.1 (17.0)	20.3 (19.5)	-	12.7 (2.0)	13.9 (2.0)	11.1 (2.0)
	Avg	20.3	20.4	-	16.5	19.3	15.1
RH [%] Year 4 (T4)	Max	62.8 (77.5)	100.0	-	83.3 (100.0)	84.9 (88.5)	88.7 (100.0)
	Min	57.8 (47.0)	100.0	-	50.9 (4.0)	40.3 (10.0)	59.8 (22.0)
	Avg	60.0	100.0	-	67.2	63.4	76.1

RH: Relative humidity, Temp: Temperature, Max/Min/Avg: yearly maximum/minimum/average value, the value in parentheses stands for the yearly peak value.

temperature and relative humidity on the properties of the specimens in these environments.

Additionally, typical records of seasonal waves of temperature and relative humidity in both outdoor and laboratory conditioning are shown in Fig. 3 for up to 4 years.

It can be noted that, in E1, despite the aim to condition the relative humidity at 55 %, it varied in the range [45–77 % RH], which can favour carbonation depth increase according to existing studies [8,11]. Besides, E5 shows increasing temperature and decreasing RH trends, while E6 shows decreasing temperature and almost constant RH trends over time. Also, higher temperatures can be noted in E5 than in E6. This shows differences in different outdoor environments.

2.3. Testing methods

2.3.1. Compression, tensile and carbonation tests of concrete

Concrete cylinders were tested to examine the E_c and the f_{cc} variation over time, using a universal testing machine (UTS) with a maximum load capacity of 2000 kN. During a non-destructive test (Fig. 4a), three LVDTs spaced at 120° were installed on the specimen to determine the E_c as per NP EN 12390–13:2013 [36]. The destructive compression test (Fig. 4b) was performed on the same specimens to determine the f_{cc} as per NP EN 12390–3:2011 [37]. A total of 90 specimens were tested for determining the E_c and the f_{cc} variations for up to 4 years. The pull-off tests were manually performed on specimens (Fig. 4c) using the DYNA Z5 testing machine (Fig. 4d) to determine the f_{ct} as per EN1542:1999 [38]. A total of 104 tests were performed to determine the variation for up to 4 years. On the other hand, carbonation tests were also performed on 52 specimens using phenolphthalein indicator to examine the evolution of the C_d over time.

2.3.2. Tensile tests of epoxy adhesives and CFRP laminates

The MTS UTS machine (Fig. 5a) was used for testing both epoxy adhesives and CFRP laminates. This MTS is additionally equipped with DIC (Fig. 5b) that helped in visualizing real-time strain evolution. Direct tensile tests of 125 epoxy adhesive specimens (Fig. 5c) were performed as per EN ISO 527–2:2012 standard [39] to determine the f_a. The E_a was determined as per EN ISO 527–2:2012 [39] by calculating the slope of the secant line on the stress-strain curve from 0.05 % to 0.25 % of the strains. Similarly, testing of 150 CFRP laminate specimens (Fig. 5d) was carried out as per ISO 527–5:2009 [40] standards to determine both the f_f and E_f.

2.4. Single lap shear tests

A total of 50 concrete prisms each with 400×200×200 [mm] were strengthened according to EBR technique using 2 CFRP laminates, each with a cross-section of 50×1.2 [mm], being applied to two opposing sides (each in the side parallel to the casting direction) of each specimen. A bond length of 220 mm was adopted for each specimen, with 100 mm free from the extremity of the concrete prism to prevent the unwanted premature failure by concrete rip-off ahead of the loaded end. The used bond length was higher than the theoretical effective length, l_e, of 101 mm, as per [41]. The geometry and dimensioning of the EBR specimens and its test set-up are shown in (Fig. 6a), followed by a picture of the test setup (Fig. 6b), where further details are given as follows: i) the horizontal and vertical restraints, and the fixation of the LVDTs supports (Fig. 6c), ii) mounting of LVDTs (Fig. 6d) and, iii) checking of the alignment and flatness of the specimen and the clamp (Fig. 6e). A total of 100 direct single-lap shear tests were performed using a servo-controlled equipment. The applied force was measured through a load cell of 200 kN maximum load carrying capacity (linearity error of 0.05 % F.S.) placed between the actuator and the grip (used to pull the CFRP laminate during the test (Fig. 6b)).

The tests were performed under displacement control at the loaded end with a rate of 2 μm/s, the displacement being measured through LVDT placed at the loaded end section (LVDT1 in Fig. 6a) as a control variable. The displacement at the free end was also recorded using the LVDT denoted as LVDT2 in Fig. 6a.

3. Results and Discussion

The results from the tests of bond constituent materials (concrete, epoxy adhesive, and CFRP laminate) are first presented and discussed, followed by those from the single-lap shear test performed on the specimens strengthened using EBR technique.

3.1. EBR CFRP-to-concrete bond constituent materials

The results from concrete, epoxy adhesive and CFRP laminate testing are presented and discussed.

3.1.1. Concrete

The results from the tests conducted on the concrete specimens are shown in Fig. 7a and Table 3. The concrete carbonation depth (C_d) increased linearly with time in E1 mainly because of the relative humidity range [50–70 %RH] known to favour the ingress of CO_2 [42], while in E3 and E4 it mainly decreased over time. In general, trends with lower values of C_d can be noted from E2 and E4. This agrees with the

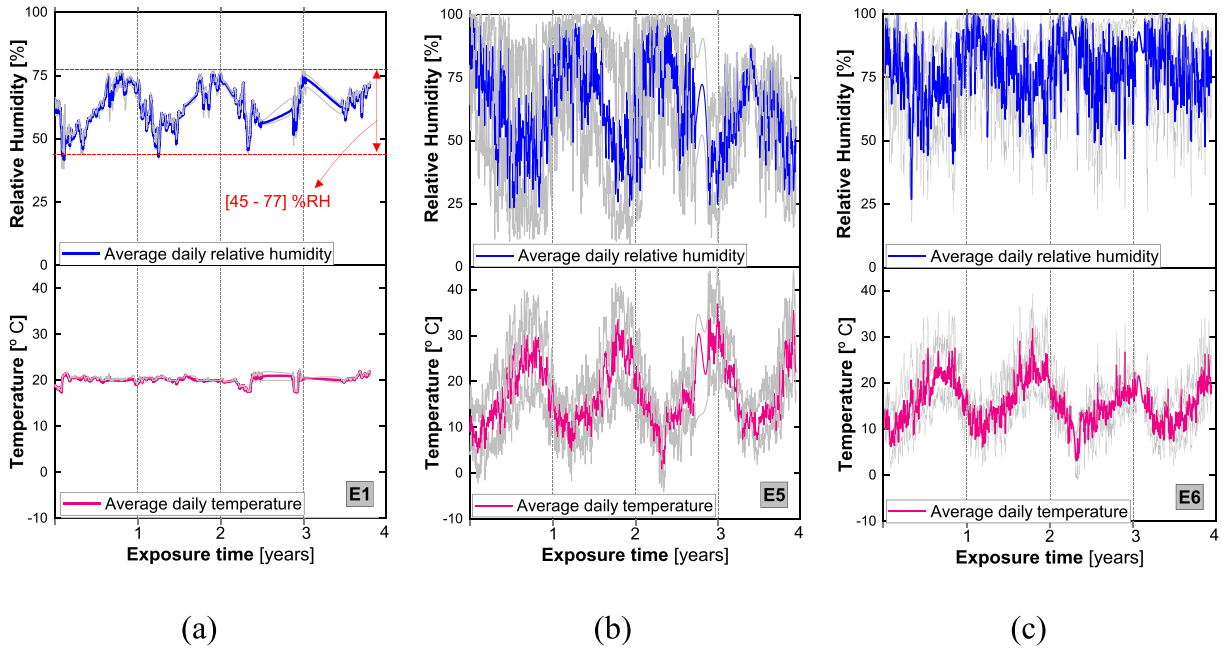

Fig. 3. Typical meteorologic records collected from (a) laboratory environment (E1) and from (b, c) outdoor environments (E5 and E6).

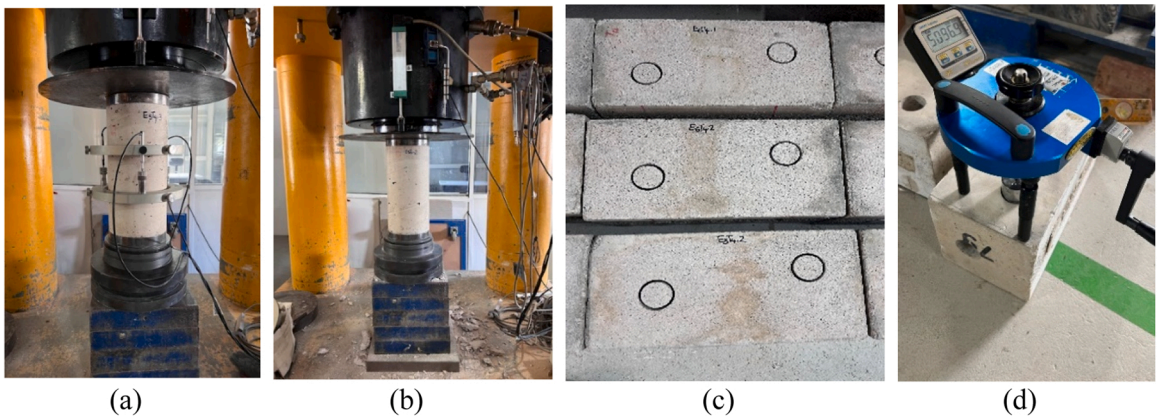

Fig. 4. Tests for characterization of concrete: (a) elastic modulus, (b) compression, and (c) sandblasting the concrete surface and creating circular grooves for bonding the metal dollies, and (d) concrete pull-off test setup.

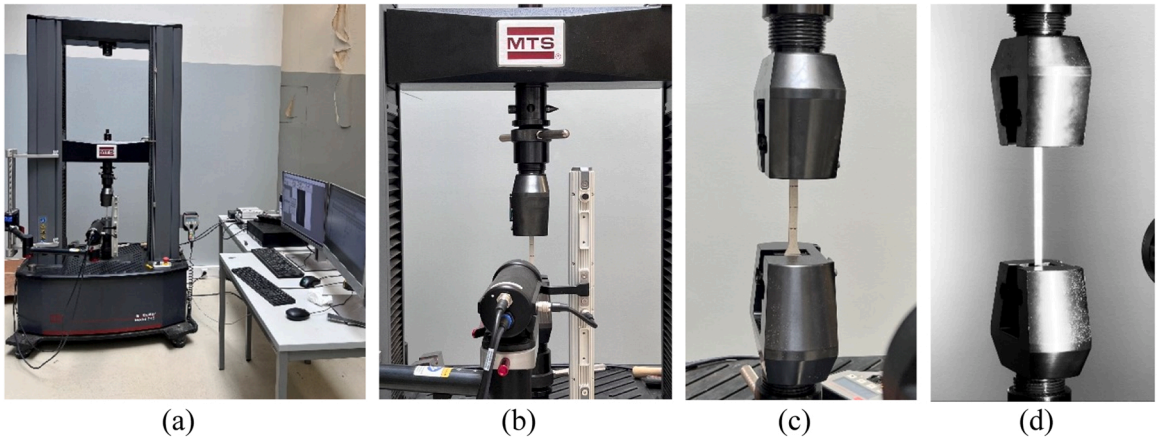

Fig. 5. Tensile tests using MTS UTS: (a) overview of the MTS equipment, (b) DIC camera used in the tests, (c) an epoxy adhesive specimen, (d) CFRP laminate specimen.

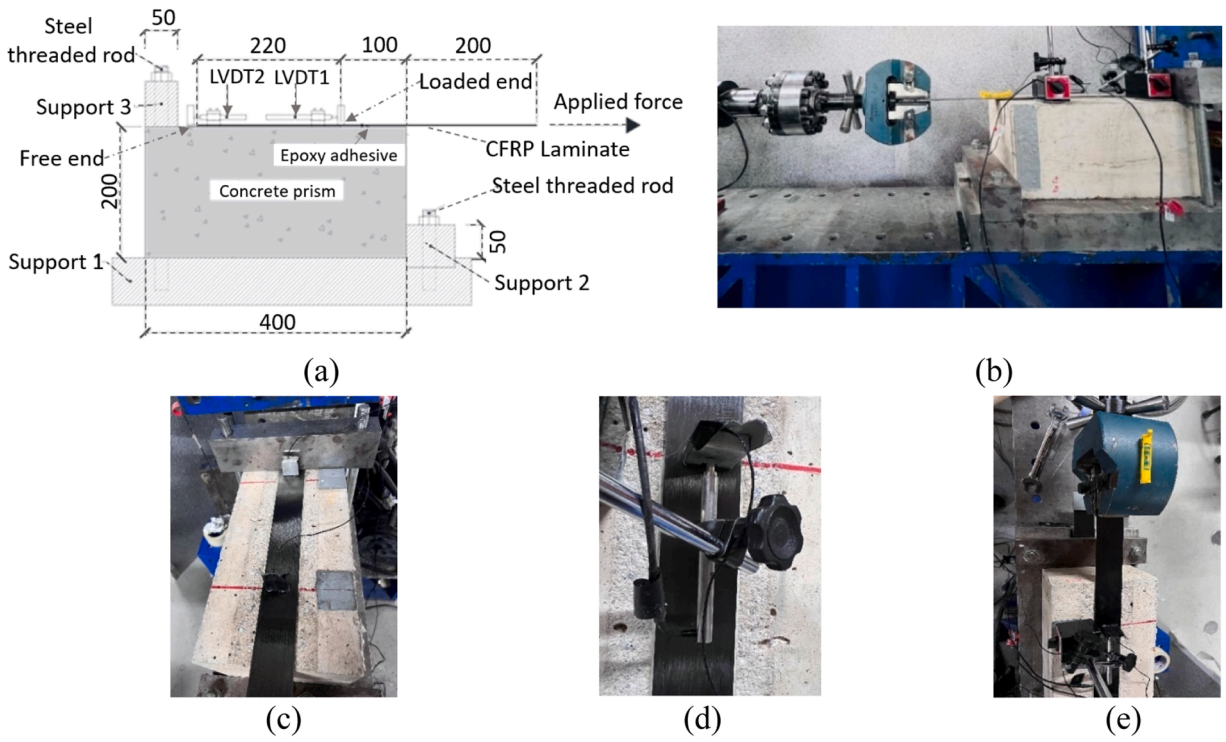

Fig. 6. Single-lap shear tests: (a) specimen's geometry and test set-up, (b) photograph of the full test configuration, (c) mounting LVDTs supports, (d) mounting LVDTs and (e) verification of the clamp and CFRP alignment. Note: all units in [mm].

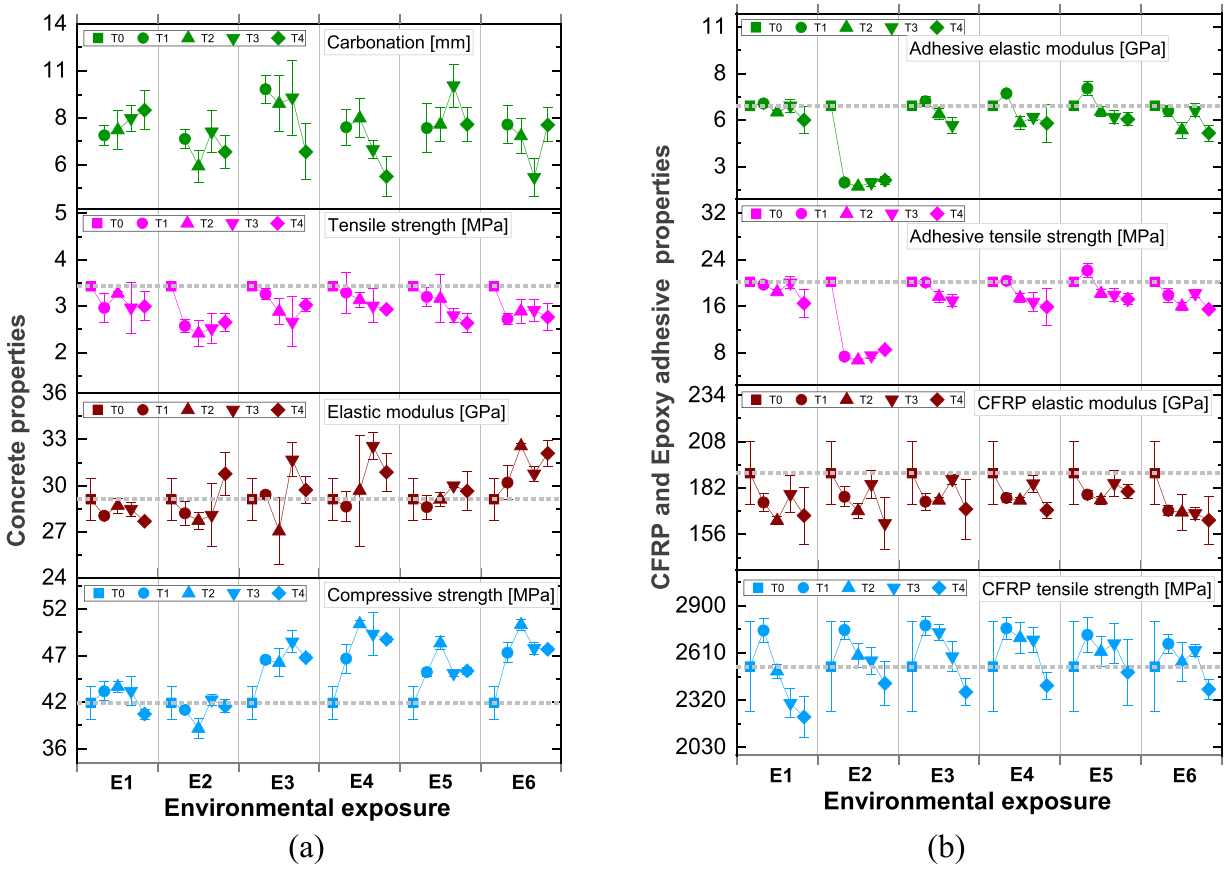

Fig. 7. Variation of the bond constituent material properties with time under different environmental exposures: (a) concrete, and (b) epoxy adhesive and CFRP laminate.

Table 3
Average values of concrete compressive strength, elastic modulus, splitting tensile strength, and carbonation depth before exposure (T0), and after 1 (T1), 2 (T2), 3 (T3), and 4 (T4) years of different environmental exposures (E1 to E6).

Environment	T0	T1	T2	T3	T4	T0	T1	T2	T3	T4
	Compressive strength f_{cc} [MPa]					**Elastic modulus E_c [GPa]**				
REF	41.5 (4.4)	-	-	-	-	29.1 (5.0)	-	-	-	-
E1	-	42.8 (2.4)	43.3 (1.4)	42.8 (3.8)	40.3 (1.4)	-	28.0 (0.7)	28.7 (1.7)	28.5 (1.6)	27.7 (0.4)
E2	-	40.7 (0.7)	38.7 (2.9)	41.9 (1.5)	41.1 (1.8)	-	28.2 (2.8)	27.7 (2.0)	28.1 (7.2)	30.8 (4.5)
E3	-	46.3 (0.9)	46.0 (3.4)	48.4 (2.5)	46.6 (0.6)	-	29.4 (0.8)	27.0 (8.0)	31.7 (3.4)	29.7 (2.9)
E4	-	46.5 (3.4)	50.3 (0.8)	49.2 (4.8)	48.6 (0.7)	-	28.6 (3.4)	29.7 (12.1)	32.6 (2.7)	30.9 (4.0)
E5	-	44.9 (1.0)	48.2 (1.5)	44.8 (0.7)	45.1 (0.9)	-	28.6 (2.6)	29.1 (1.6)	30.0 (0.3)	29.6 (4.2)
E6	-	47.1 (2.4)	50.2 (1.3)	47.6 (1.4)	47.5 (0.5)	-	30.2 (3.7)	32.6 (0.5)	30.8 (1.5)	32.1 (2.6)
	Pull-off strength f_{ct} [MPa]					**Carbonation depth C_d [mm]**				
REF	3.4 (13.3)	-	-	-	-	0.0	-	-	-	-
E1	-	2.9 (10.4)	3.2 (1.3)	2.9 (18.4)	2.9 (10.5)	-	7.4 (19.9)	7.7 (14.8)	8.4 (9.2)	8.9 (12.8)
E2	-	2.5 (5.3)	2.3 (11.8)	2.5 (13.1)	2.6 (7.4)	-	7.2 (15.2)	5.5 (17.7)	7.6 (16.4)	6.4 (15.3)
E3	-	3.2 (3.6)	2.8 (9.7)	2.6 (20.1)	3.0 (4.7)	-	10.1 (5.5)	9.3 (18.2)	9.6 (23.4)	9.0 (18.8)
E4	-	3.2 (13.5)	3.1 (5.3)	2.9 (12.2)	2.9 (0.1)	-	7.8 (7.5)	8.4 (14.1)	6.5 (8.4)	4.9 (24.1)
E5	-	3.1 (6.3)	3.1 (16.4)	2.7 (5.7)	2.6 (7.7)	-	7.8 (10.9)	8.0 (12.5)	10.3 (12.4)	8.0 (12.5)
E6	-	2.7 (4.4)	2.8 (8.8)	2.9 (8.1)	2.7 (10.5)	-	8.0 (14.1)	7.3 (13.9)	4.9 (22.9)	8.0 (12.8)

Note: all values in parentheses are *coefficients of variation*, REF: Reference values from the specimens tested at T0.

findings by [43] where an increased humidity, rain, and snow was reported to slow the ingress of CO_2 after exposing concrete to outdoor environments for up to 4 years. In E2 and E4 the specimens were partially carbonated (Fig. 8a), hence having negligible effects on the concrete properties [44,45]. The highest C_d was observed in E3 as expected. However, even in other outdoor environments (except E4) the C_d was observed to be comparable to that in E3, which reflects the abundance of CO_2 everywhere in the atmosphere; the highest average values of C_d of 9.5 mm and 8.5 mm are found in E3 and E5, respectively.

The concrete compressive strength (f_{cc}) increased in all outdoor environments as compared to the value recorded at initial time T0. In E1, the f_{cc} increased from T0 to T2 by 4.3 % and decreased from T3 to T4 by 6.2 %. In E2, the f_{cc} decreased from T0 to T2 by 7.2 % followed by an increase from T2 to T3 by 8.3 % and levelled off thereafter. The observed increase can be thought to have resulted from the continuation of cement hydration with time, which increased the number of C-S-H silicates that occupied the empty voids, thereby reducing the porosity and improving the strength. The increase in the C-S-H silicates is already known to improve the f_{cc} [46,47]. Furthermore, since carbonation increases the f_{cc} [12,15], this can confirm the increased f_{cc} in E3 as a result of high carbonation. Also, increased curing humidity was found to increase the f_{cc} and E_c by [14]. Hence, the increased f_{cc} in E4 can be attributed to the effect of freeze-thaws that promoted the continuation of cement hydration, which is in line with the findings by [48].

Briefly, the continuation of cement hydration in E4 and E6 with the presence of high outdoor humidity can be thought to have been the main governing factor of the increased concrete f_{cc} and E_c. Furthermore, the observed increase in E6 may further be attributed to the synergic effect between carbonation and chlorides. In E5, elevated temperatures as previously shown in Fig. 3 led to increased f_{cc}, which agrees with a study by [49], also, elevated temperatures have been found to make concrete more porous thereby facilitating the CO_2 penetration [8–10]. Since there was a high C_d in E5 (Fig. 7a), it can be inferred that the increased f_{cc} resulted from a synergic effect between elevated temperatures and carbonation. On the other hand, the f_{ct} showed a decreasing trend over time. It is worth noting that pull-off tests are also usually used to characterise FRP-to-concrete systems; despite that, they may not accurately represent the mechanisms occurring at the concrete near-surface region in FRP strengthened RC structural elements. Overall, the highest increases in outdoor environments were approximately 21 %, 16 %, 21 %, and 17 % in the f_{cc}, and 9 %, 12 %, 3 %, and 12 % in E_c for E3, E4, E5, E6, respectively. Typical FMs for both concrete compression and pull-off tests are shown in Fig. 8b and Fig. 8d, respectively. The FM from the compression tests are as per NP EN 12390–3:2011 [37]. Furthermore, the FM is of cohesive failure in deeper regions of the concrete, from which it can be inferred that the pull-off force at such a failure may not be the actual representation of that leading to failure at concrete near-surface region (i.e., the region of interest, as it is where the CFRP is bonded).

3.1.2. *Epoxy adhesive*

The results from the tensile test of the epoxy adhesive are shown in Fig. 7b and Table 4. Referring to Fig. 7b, and Table 4, marginal changes in both adhesive elastic modulus (E_a) and its strength (f_a) can be noted in E1. Contrary, there was a substantial decrease in both E_a and f_a in E2. This decrease can be attributed to the effects of plasticization. Furthermore, a general progressive decrease in E_a during the later years can be noted in all environments. A similar trend for f_a and E_a can be seen in all environments, which shows that predictive models considering both the f_a and E_a trends can reasonably be developed. The highest decreases in E_a and f_a were 75.4 % at T2 and 66.3 % in E2 at T2, respectively, as compared to the value at initial stage (T0).

The justifications for the observed reductions in the adhesive properties can be as follows: (i) the observed marginal variations in E1 resulted from carbonation that may have caused the epoxy resin to cure faster [23]; (ii) water ingress in E2 and moisture effects in both E4 and E6 were the main degradation agents, as also found by [17,18]; (iii) In E3, synergic effects between elevated temperatures, carbonation, and

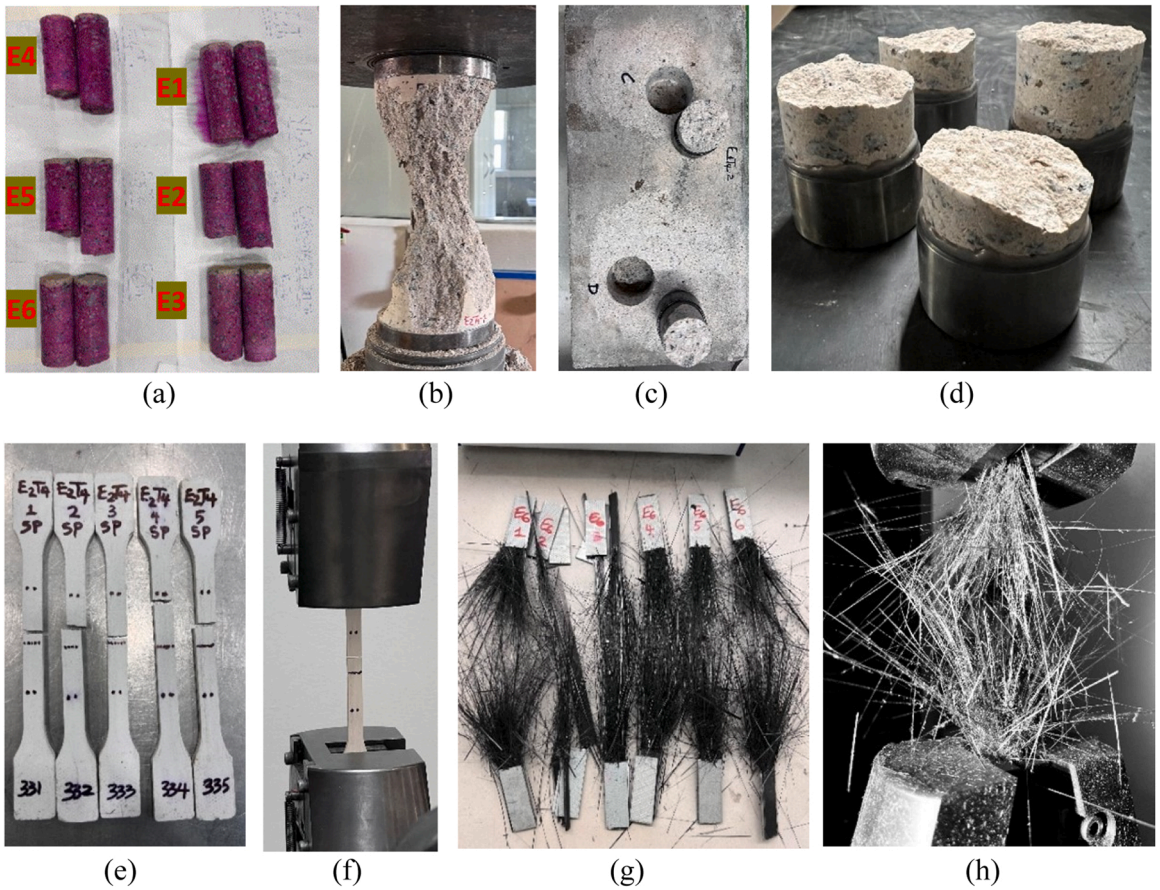

Fig. 8. Typical aspects/failure modes of some specimens after testing: (a) carbonation of concrete after T4; (b) concrete under compression, (c,d) concrete under tension (pull-off), (e,f) epoxy adhesive, and (g,h) CFRP laminate under tension.

UV radiations can be thought to be the main agents; iv) synergic effects between elevated temperatures and carbonation; and iv) a slight decrease observed in E6 can be attributed to moisture effects mainly because chlorides effects on epoxy adhesive are negligible [22]. The adhesive failure modes (Fig. 8e) were of an abrupt break in the region of the tensioned adhesive part (Fig. 8f). The adhesive tensile strains are also shown in Table 4. Marginal variations with time can be noted, except in E2 where the specimens showed a substantial increase during T1 followed by a level-off in the later years.

3.1.3. CFRP laminate

The results from the tensile test of the CFRP laminate are shown in Fig. 7b and Table 4. The CFRP laminate tensile strength (f_f) generally improved in the first year in all environments, while its elastic modulus (E_f) showed a progressive decrease as compared to the initial value at T0. The highest f_f occurred at T1 which reflects the effects of post-curing of the fibre resin matrix, followed by a general decrease in the consecutive years. After 4 years of exposure, in comparison with the initial value (T0), the f_f showed a decrease of 12.3 %, 4.2 %, 6.3 %, 4.7 %, 1.4 %, and 5.6 % in E1 to E6, respectively, while the E_f showed a decrease of 12.6 %, 14.7 %, 10.5 %, 10.5 %, 5.3 %, and 13.7 % in E1 to E6, respectively. These variations show that E_f degradation was faster than that of the f_f. The failure modes were characterized by a quick and progressive rupture of individual fibres that started from the CFRP longitudinal edges and moved towards the centre until the complete failure occurred with a massive sound (Fig. 8g,h). The improved CFRP properties in E1 may have resulted from the post-curing of the resin, mainly catalysed by the presence of carbonation that caused the epoxy resin to cure faster, as was observed in [23]. In E2, the observed marginal variations indicate that f_f was immune to water diffusion; however, its E_f was remarkably affected. Similar trend was observed in [50] after 6 months of the CFRP laminate immersion in seawater with a reduction of its elastic modulus from 248.5 GPa to 240.5 GPa, hence water diffusion through the laminate may be thought to affect the elastic modulus but with insignificant effects on the tensile strength. In E3, both carbonation and high temperatures may have led to a higher resin matrix post-curing rate during T1; however, the curing rate reduced in the later years, which led to decreasing f_f trends. In E4, the post-curing rate was also high during T1 and then slowed down thereafter, which allowed the freeze-thaws to start causing fibre matrix microcracks and progressively decreasing the f_f, this agrees with the findings by [25]. In E5, a synergic effect between high temperatures and the presence of carbonation can be attributed to the observed increased f_f with marginal decrease after 4 years. Furthermore, in E6 chlorides do not affect the CFRP properties [18], hence, the post-curing rate during T1 was favoured by carbonation, but the rate was outweighed by the moisture effects in the later years. Finally, the maximum CFRP strain evolution are also shown in Table 4, and a general increase as compared to the value at T0 can be noted.

3.2. EBR CFRP-to-concrete bond

3.2.1. Pull-out force versus loaded end slip curves

The relationships between the pull-out force and the loaded end slip from T0 to T4 are shown in Fig. 9a-f for the studied environments (E1-E6), respectively. Additionally, the average maximum pull-out forces achieved during tests are shown in Table 5. For more details, the maximum force-slip values and the force-slip curves for each tested specimen are shown in Annex I and II, respectively. It can be noted that the pull-out force and slip changed from year to year in each

Table 4
Average values of epoxy adhesive and CFRP tensile strength, elastic modulus, maximum tensile strain before exposure (T0), and after 1 (T1), 2 (T2), 3 (T3), and 4 (T4) years of different environmental exposures (E1 to E6).

	T0	T1	T2	T3	T4	T0	T1	T2	T3	T4
Environment	**Epoxy adhesive: Tensile strength [MPa]**					**CFRP laminate: Tensile strength [MPa]**				
REF	19.9	-	-	-	-	2527	-	-	-	-
	(3.0)					(11)				
E1	-	19.5	18.2	19.8	16.3	-	2748	2497	2302	2217
		(1.8)	(2.8)	(4.9)	(14.6)		(2.6)	(1.7)	(3.9)	(5.7)
E2	-	7.2	6.7	7.4	8.4	-	2750	2594	2562	2422
		(3.1)	(2.7)	(7.1)	(3.6)		(2.0)	(2.8)	(3.2)	(5.6)
E3	-	19.9	17.4	16.7	-	-	2778	2735	2587	2369
		(3.1)	(5.3)	(5.9)			(2.1)	(1.8)	(3.6)	(3.6)
E4	-	20.1	17.2	16.5	15.7	-	2760	2703	2690	2409
		(3.4)	(4.3)	(9.8)	(20.1)		(2.5)	(3.4)	(2.9)	(3.5)
E5	-	21.9	18.0	17.7	17.0	-	2720	2618	2667	2491
		(5.2)	(3.6)	(6.5)	(5.8)		(3.9)	(3.6)	(4.6)	(8.1)
E6	-	17.7	15.8	18.0	15.3	-	2665	2554	2626	2386
		(6.4)	(4.3)	(4.2)	(2.6)		(2.2)	(4.6)	(1.3)	(2.6)
	Epoxy adhesive: Elastic modulus [GPa]					**CFRP laminate: Elastic modulus [GPa]**				
REF	6.5	-	-	-	-	190	-	-	-	-
	(3.0)					(9.3)				
E1	-	6.6	6.1	6.5	5.6	-	174	164	179	166
		(1.3)	(1.4)	(6.0)	(14.6)		(2.8)	(1.3)	(5.9)	(9.7)
E2	-	1.9	1.6	1.9	2.0	-	177	169	184	162
		(5.1)	(4.0)	(14.6)	(12.4)		(3.2)	(2.3)	(4.3)	(8.9)
E3	-	6.7	6.0	5.3	-	-	174	175	187	170
		(4.4)	(5.4)	(8.9)			(3.6)	(0.9)	(1.5)	(10.0)
E4	-	7.2	5.4	5.8	5.4	-	176	175	184	170
		(1.4)	(6.9)	(4.0)	(21.1)		(1.5)	(0.8)	(2.6)	(2.6)
E5	-	7.5	6.1	5.8	5.7	-	178	175	185	180
		(5.7)	(5.0)	(6.5)	(7.0)		(1.2)	(1.3)	(4.1)	(2.2)
E6	-	6.2	5.0	6.2	4.8	-	169	168	168	164
		(5.4)	(10.0)	(6.2)	(10.0)		(1.6)	(6.0)	(1.9)	(8.2)
	Epoxy adhesive: Tensile strain [%]					**CFRP laminate: Maximum tensile strain [x10^{-3}]**				
REF	0.4	-	-	-	-	13.3	-	-	-	-
	(6.2)					(13.6)				
E1	-	0.4	0.3	0.3	0.4		15.8	15.3	12.9	13.7
		(13.0)	(11.7)	(8.8)	(11.3)		(3.6)	(1.9)	(6.3)	(5.5)
E2	-	1.1	1.1	1.0	0.9	-	15.6	15.4	13.9	14.6
		(21.4)	(11.9)	(25.5)	(15.3)		(3.9)	(3.0)	(3.9)	(2.6)
E3	-	0.3	0.3	0.3	-	-	16.0	15.6	13.6	14.7
		(11.1)	(19.1)	(10.1)			(3.6)	(1.2)	(4.9)	(5.1)
E4	-	0.3	0.3	0.3	0.3	-	15.7	15.4	14.6	15.0
		(11.3)	(12.8)	(24.6)	(24.8)		(2.8)	(3.3)	(1.6)	(4.4)
E5	-	0.3	0.4	0.3	0.4	-	15.3	14.9	14.5	15.1
		(11.2)	(13.1)	(11.5)	(10.5)		(4.1)	(2.6)	(7.7)	(6.0)
E6	-	0.3	0.3	0.3	0.4	-	15.7	15.2	15.7	14.8
		(4.3)	(12.9)	(17.4)	(14.2)		(2.6)	(6.1)	(2.6)	(8.2)

Note: all values in parentheses express *coefficient of variation* in percent, the CFRP laminate had a 50×1.2 [mm] cross-section (during testing coupons of 15×1.2 [mm] section was used), REF: Reference values at the beginning i.e., at T0.

environment. There was also a significant change in the stiffness that depended on the exposure time and type. Because of these changes in both the pull-out force, slip and stiffness, an attempt to establish the relationship between the variation of the maximum force and the slip as time passes was carried out. In fact, it can be noted from Fig. 9a-f that after the maximum pull-out force attained its maximum there was a rapid increase of the loaded end slip with slight variation in the pull-out force, hence a tendency to form a plateau of which its length was controlled by the loaded end slip (i.e., the slip measured from the point corresponding to the maximum pull-out force, to the end or ultimate slip). However, due to change in the force from time (year) to time (year), the starting point of the above-mentioned plateau also changed thereby possessing a varying height (from the location of the minimal value of the maximum force to that of maximal value). This varying height is denoted as the *plateau height*. Similary, the slip from the point (location) where the maximum pull-out force occurred to the end of the formed plateau also changed with time of ageing, and with the plateau height, hence possesing a varying length (width) over time, denoted as *plateau width*. A comparative plot on the *plateau height* and *plateau width* is presented (see Fig. 9g) and more explanation is given as follows.

The *plateau height* in E2 and E6 decreased significantly as compared that at T0, followed by that in E5 and E3, which indicates that bond-slip curves' stabilization was faster in these environments as compared to that in E1 and E4. Mainly, water or chlorides ingress reduced the dispersion of the pull-out force with time, which therefore can help in developing better predictions over a long-term period. Furthermore, the lowest plateau width was found in E2 followed by E4, thereby indicating that the effective bond length was significantly affected by water immersion and freeze-thaws. The plateau width in E2 decreased by approximately 25 %, while that in E4 decreased by 19%, as compared to that at T0. According to [51], 200 and 500 freeze-thaw cycles decreased the bond length by 3 and 9 % respectively, hence the effects of 200 and 500 freeze thaw cycles may represent 4 yearly outdoor (natural) freeze thaw attacks if multiplied by a certain matching factor. Other studies have also showed that freeze-thaw cycles will reduce the effective bond length [52]. Also, in a study by [24], the effective bond strength decreased by 1.5 % due to thermal cycles in air, which agrees with the observed decrease in the plateau width in E5. On the other hand, the maximum pull-out force (F_{max}) and its standard variation is shown in Fig. 9h for all environments from T0 to T4. For outdoor exposures, it can

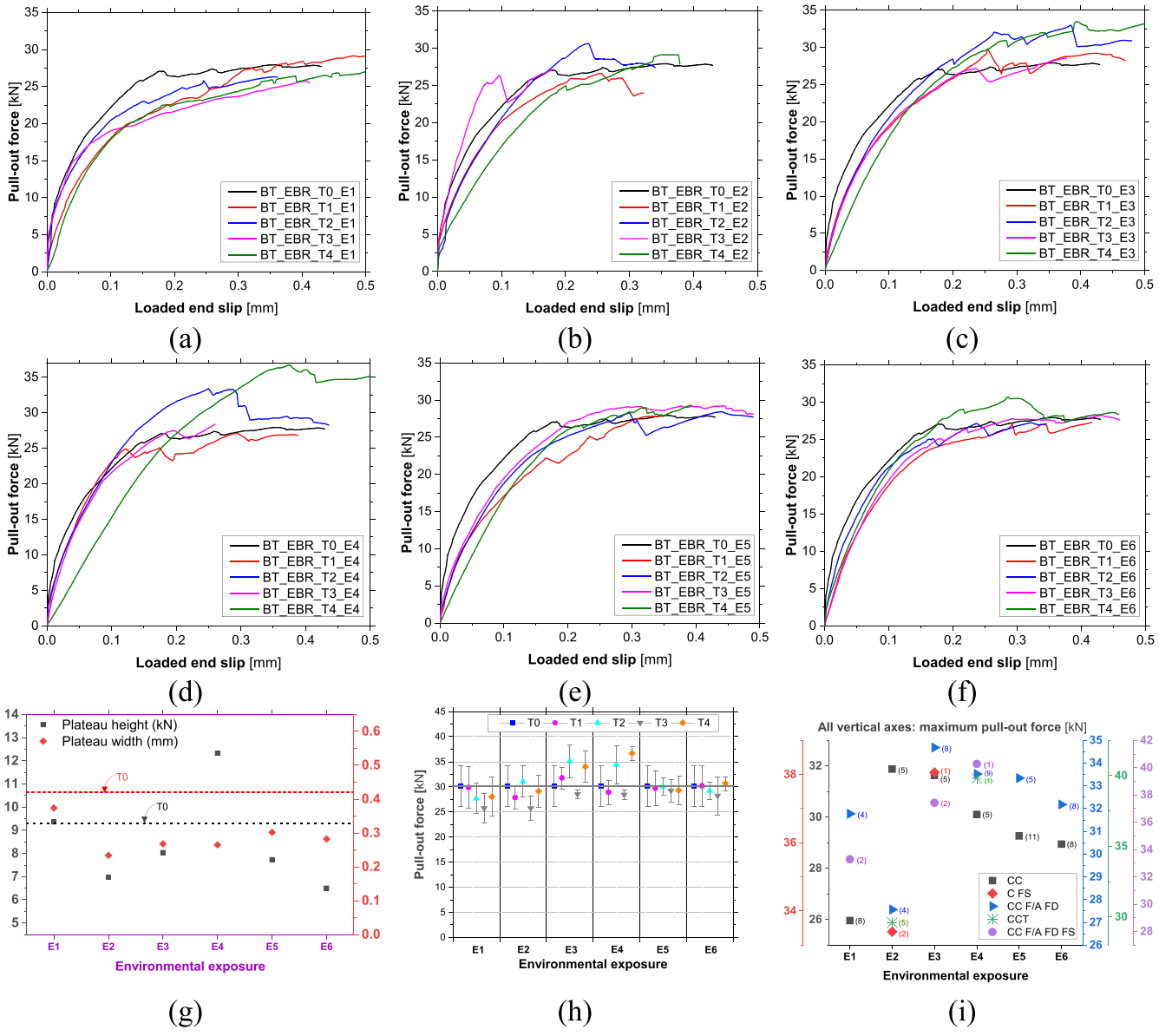

Fig. 9. EBR CFRP-to-concrete bond test results: (a-f) pull-out force *vs.* loaded end slip, (g) plateau width and plateau height variations, (h) maximum pull-out force (F_{max}) variation, (i) failure modes variability with environment and F_{max}.

Table 5
Maximum pull-out force and initial stiffness values for all studied environments for up to 4 years (each value is the average of four tests).

Environment	Maximum pull-out force F_{max} [kN]					Initial stiffness [kN/mm]				
	T0	T1	T2	T3	T4	T0	T1	T2	T3	T4
REF	30.2 (13.3)					299.4				
E1	-	29.88 (13.8)	27.67 (11.0)	25.74 (10.9)	28.05 (13.2)	-	252.6	284.8	278.7	228.5
E2	-	27.86 (8.4)	31.06 (10.0)	27.18 (8.6)	29.14 (9.5)	-	230.0	220.8	336.4	165.6
E3	-	31.78 (6.7)	35.10 (9.1)	28.56 (3.0)	34.02 (8.8)	-	281.4	221.0	232.2	181.3
E4	-	28.92 (8.4)	34.40 (11.1)	28.41 (3.4)	36.70 (3.7)	-	243.4	232.5	299.4	152.2
E5	-	29.71 (11.5)	30.10 (5.9)	29.24 (7.3)	29.28 (9.2)	-	270.0	191.8	192.4	172.1
E6	-	30.21 (13.5)	29.23 (6.0)	28.23 (12.4)	30.68 (4.3)	-	254.9	261.1	235.1	252.5

Note: all values in parentheses express *coefficient of variation* in percent; REF: Reference values at the beginning i.e., at T0

be noted that E3 and E4 showed significant variations with increasing tendency, while E5 and E6 showed marginal variations with stabilizing tendency. Furthermore, the laboratory conditioning (E1 and E2) showed insignificant variations, but with a decreasing tendency.

3.2.2. Failure modes

Failure modes at T0: At the initial time (T0), four specimens were tested and two failed by concrete cohesive (CC) failure (Fig. 10a,c) while the remaining two showed a mixed failure (Fig. 10b,d). Two reasons can be attributed to these failures. First, the CC failure may demonstrate that the concrete was the weakest part probably because of the incomplete cement hydration, or due to its lower strength as compared to other bond constituent materials. Second, the mixed failure mode may indicate that adhesive joint was not yet fully cured with relatively low cross-linking degree.

Failure modes after exposure: It can be noted that generally either CC or a mixed failure of concrete, adhesive and CFRP occurred (Fig. 10.e-j). More details on these failures are provided in Fig. 10.k-n, where the CCT denotes the CC failure with a thick layer of concrete detached at free end region; F/A denotes the adhesive failure, FD denotes the CFRP disbond, and FS denotes the CFRP splitting/fracture. For example, a mixed failure mode denoted as "CC F/A FD" indicates that the specimen failed by the concrete cohesive failure in some bonded regions, the adhesive failure and the CFRP disbond in other regions (example of this type of failure is shown in Fig. 10h). The failure mode denoted as "CC F/A FD FS" indicates the mixed failure defined above for "CC F/A FD" but also with CFRP splitting (i.e., a failure like that one shown in Fig. 10h but with CFRP longitudinal splitting shown in Fig. 10m as FS).

Visual observations led to noting that concrete region with fewer aggregates was more likely to fail before that with more aggregates,

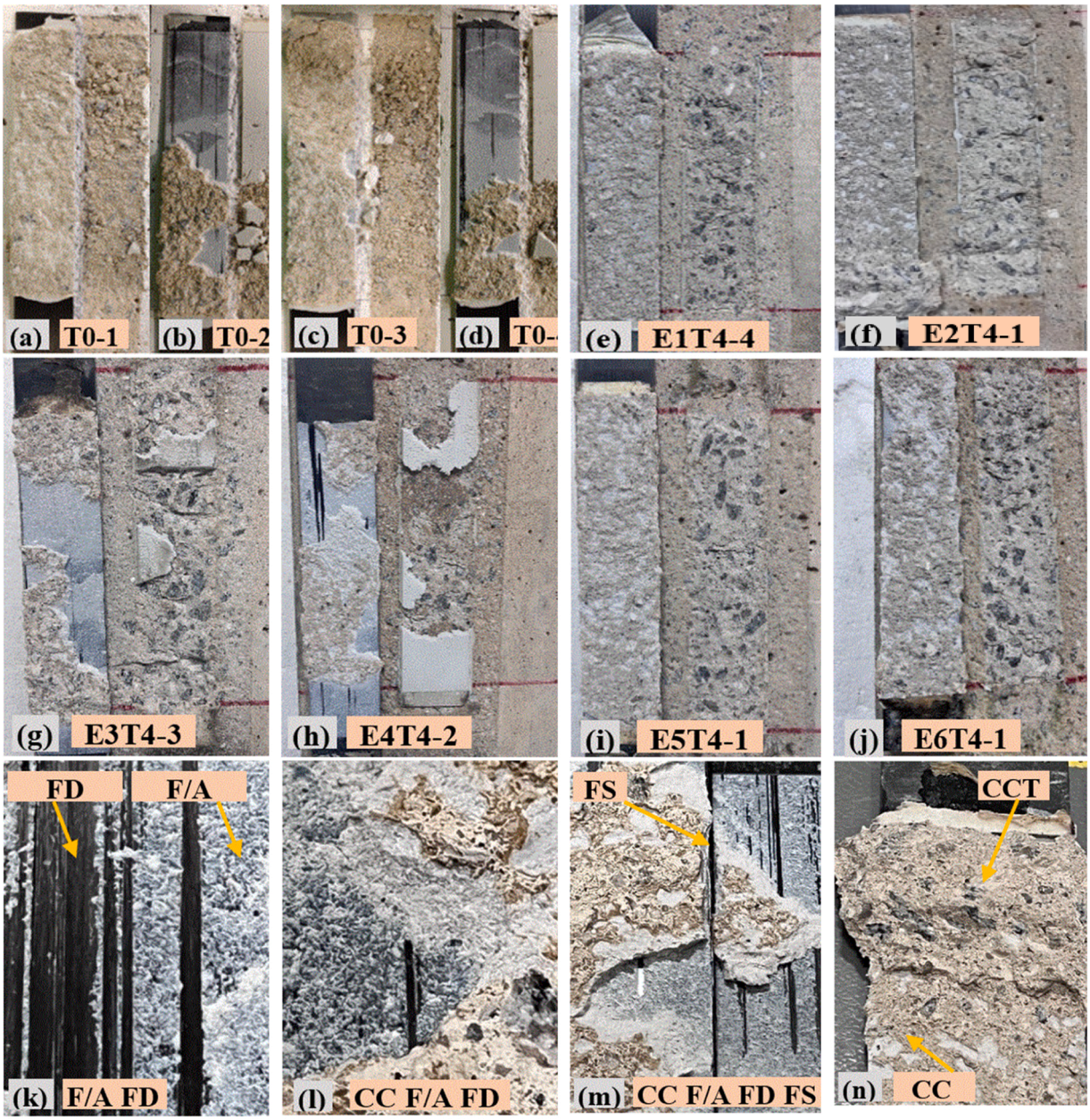

Fig. 10. Failure modes of EBR CFRP-to-concrete bond: (a-d) failure modes before exposure: concrete cohesive (CC) in T0-1 and T0-3, and mixed failure in T0-2 and T0-4 specimens; (e-j) typical predominant failure modes after exposure in each environment (E1 - E6): (e,i,j) concrete cohesive (CC), (f) CC with a thick layer at free end (CCT), (g,h) mixed failure (CC F/A FD) i.e., CC mixed with adhesive failure (F/A) and CFRP disbond (FD); (k-n) main regions (i.e., FD, F/A, FS, CC, and CCT) of the failures shown in (a-j) together with their corresponding notations used in text and in Fig. 9i. FS is when the CFRP laminate fractured in the longitudinal direction.

hence resulting in the higher pull-out force in the latter. Furthermore, the mixed failure mode generally led to higher pull-out force than the sole CC (Fig. 9i). This former failure occurred probably due to the adhesive being bonded to concrete with unequal distribution of aggregate at the concrete near-surface region, which caused unequal distribution of stresses, eventually leading to concrete failures in some regions (i.e., regions with fewer aggregates) and adhesive failures in other regions (i.e., regions of adhesive bonded to concrete with more aggregates). The mixed failure may also reflect the degradation of the materials themselves as time passes. It is worth noting that existing models for the CFRP-concrete bond generally consider the CC failure [53] without including other types of failure mode such as those observed in this work, hence further improvements by incorporating all types of failure modes can be crucial.

3.3. Constituent materials versus EBR CFRP-concrete bond properties

In this section, the change of EBR CFRP-to-concrete bond properties with time, in each studied environments, are analysed taking into consideration of effects of the change of properties of the materials constituting the bond. The bond properties considered are the bond strength and bond stiffness. The former was obtained directly from the pull-out tests, while the latter was derived from each of the pull-out force *vs* loaded end slip curve by performing a linear fitting considering the force range between 0 and 10 kN.

Bond strength variation in E1: The pull-out force consistently decreased from T0 to T3 and then increased from T3 to T4; however, the value at T4 was still lower than that at T0. Also, the bond stiffness generally showed a decrease. The lowest bond strength and bond stiffness retentions were around 0.9 at T3 and 0.7 at T4, respectively, which shows that the stiffness degradation was faster than that of bond strength. As can be seen from Fig. 11a, the concrete tensile strength (f_{ct}) and the CFRP laminate tensile strength (f_f) reductions would be attributed to the observed bond strength reduction, while in Fig. 11b, the CFRP laminate elastic modulus (E_f) reduction would also be attributed to the observed bond stiffness reduction. However, since the dominant failure mode was by concrete cohesive (CC), see Fig. 9i, concrete was still the weakest part of the bond, and hence the bond strength/stiffness decrease can be due to altered concrete properties, particularly its f_{ct}, or bonding redistributions that resulted from improved properties. It is worth noting that the highest maximum pull-out force occurred from the specimens that failed by CC F/A FD FS failure as can be seen from Fig. 9i.

Bond strength variation in E2: From Fig. 11a,b, the bond strength showed significant fluctuations over time, and the bond stiffness showed a general decrease except at T3. Like what is observed in E1, the lowest bond strength and stiffness retentions were around 0.9 at T3 and 0.7, respectively, again revealing that the stiffness degraded faster than the strength. The bond strength variations can be thought of mainly be related to the degradation adhesive tensile strength (f_a) and concrete pull-off strength (f_{ct}), whereas the degradation of the bond stiffness can be attributed mainly to the E_a and E_f reductions (see Fig. 11a,b). In fact, water ingress can disrupt the interchange bonds thereby leading to plasticization effects [54]. It was shown that concrete and adhesive are bonded via chemical bond and mechanical interlock and the primary chemical interaction between the two adherends is hydrogen bonding, very weak compared to the covalent bonding [55]. The mechanical interlock will be loosened by plasticization thereby reducing the adhesive stiffness and water molecules will tend to react with the loosened interlock and breaks the hydrogen bond [55], hence leading to reduced bond properties. The predominant failure mode in E2 was CC at an average pull-out force of 32 kN and CCT at 29 kN (Fig. 9i). However, there was a tendency for the failure to be a "CC F/A FD", with a lower average force (27.5 kN) than that at CC (see Fig. 9i), thereby indicating that the negative effects of degraded f_a were more pronounced than those of degraded f_{ct}. Besides, the specimens with larger region of

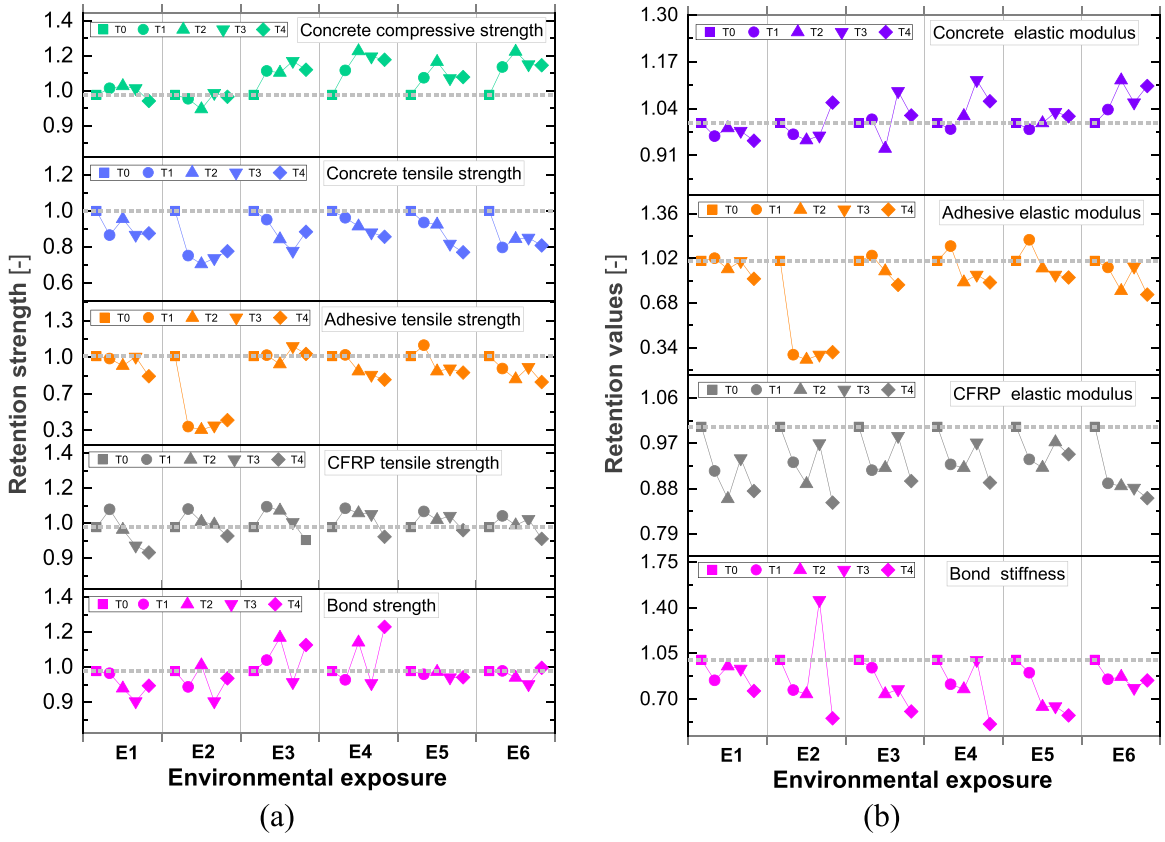

Fig. 11. Comparative perspectives on the effect of change of material properties on (a) the bond strength and (b) bond stiffness behaviour.

aggregate bonding to adhesive failed at the highest pull-out force, which confirms the significant positive effect of the aggregate bonding to the adhesive as the aggregate strength is neither affected by water nor partial carbonation.

Bond strength variation in E3: A tentative increase in bond strength is observed (Fig. 11a) which may be attributed to the post-curing of both adhesive and CFRP that increased polymer cross-linking due to high temperatures, also the post-curing was speeded up by carbonation as described in Section 3.1. Since the bond strength generally increased when the f_{cc} and f_f significantly increased with almost unchanged f_a, it seems the degraded f_{ct} had no effect on the bond strength. On the other hand, the bond stiffness showed a progressive decrease over time (Fig. 11b), the lowest retention being nearly 0.65. This decrease may have resulted from the degraded E_a and E_f, as the E_c generally did not decrease. The stiffness degradation may also be attributed to the chemical bond change at the interface with time between the concrete and adhesive (e.g., break of hydrogen bonds linking concrete to the adhesive) and/or between the adhesive and CFRP laminate (e.g., break of covalent bonds linking adhesive to the CFRP). The predominant failure mode was "CC F/A FD" (Fig. 10g), which was more beneficial compared to CC as it led to the higher average maximum pull-out force (34.5 kN). In fact, the improved concrete properties shifted the failure mode from being of the sole CC to "CC F/A FD". Also, the tensile properties of adhesive reduced, which confirms the observed predominant failure mode. Comparing all failures from T0 to T4, the maximum pull-out force (38.4 kN) occurred for the case when the failure was "CC FS" (see Fig. 9i), which shows that the FS occurrence imposed higher pull-out force, hence the failure with splitting of the CFRP laminate would be the desired failure mode. Another perspective is that the climate change led to conditioning dissimularity from year to year, hence, both the duration of exposure and the exposure severity significantly changed with time. Hence, the bond strength and bond stiffness may have depended on the above dissimilarity, where the longer the exposure the higher the variation or the more the severity the more the variation in a particulary year.

Bond strength variation in E4: The bond strength showed fluctuations with a general increasing tendency (Fig. 11a); contrarly, the bond stiffness showed a general decrease with time (Fig. 11b). The lowest bond stiffness retention was 0.51. Both the concrete E_c and f_{cc} retentions increased but with some reduction in its f_{ct}. However, both the adhesive E_a and f_a reduced. A slight reduction of the CFRP E_f and f_f was also observed. Hence, the decreased adhesive properties may have led to the observed variation of the bond properties. However, the increased cement hydration in concrete and the post-curing of the CFRP may also have caused adjustement in the bonded region which either caused the bond strength to decrease or increase. Hence, this phenomenon can also be thought to have contributed to the fluctuations observed. Another perspective aligns with that described for E3, where the conditioning dissimilarity may have contributed to the observed fluctuations. A study by [27] showed that 300 FT cycles consisting of 16 h of freezing and 8 h of thawing in water bath did not significantly damage the bond between CFRP and concrete, which agrees with the results from E4 (Fig. 11a). Also, in a study by [25], it was found that the greater the number of freeze-thaw cycles the lower the sliding stiffness and loaded end slip of the CFRP-concrete interface, which is similar to what is observed in E4 (Fig. 11b). The predominant failure mode was "CC F/A FD" at an average of pull-out force of approximately 33.5 kN, and the failure that led to the highest pull-out force was "CC F/A FD FS" with 41 kN, which shows that a mixed failure with the occurrence of CFRP splitting/-fracture can be suggested to be the desired failure mode. In general, the pull-out force increased for mixed failure (Fig. 10h) as compared to when there was a sole CC. Also, the larger the CFRP-adhesive interface failure region the higher the pull-out force. Mixed failure modes were also reported in [56,57]. The combined effects of freeze-thaw attacks and the UV exposure can be thought to have taken place which resulted in some CFRP fracture/splitting failure, i.e., the microcracks may have formed thereby allowing the entrance of UV that caused more harmaful effects to the fibre matrix. This agrees with the findings by [30]. Hence, the damaged fibre matrix is likely to be attributed to the observed mixed failure mode, particularly that containing FD or FS or both.

Bond strength variation in E5: A stable and slightly decreasing trend in the bond strength is observed (Fig. 11a). This trend can show the competing mechanisms between the temperature effects on the matrix post-curing for both CFRP and adhesive, and concrete carbonation or cement hydration effects (or other effects such as UV radiation) all of which tend to balance each other over time. However, the bond stiffness showed a progressive decrease over time (Fig. 11b), the highest decrease being 39%, which indicates that the stiffness degraded faster than the bond strength. The stiffness decrease with increased temperature was also reported in a study by [28]. In fact, the increase in f_{cc} and f_f may have neutralized the negative effects from the degraded concrete f_{ct} and the f_a (Fig. 11a), thereby leading to marginal changes of the bond strength. On the other hand, the bond stiffness degradation can be attributed to the degraded E_f and the E_a (Fig. 11b). The CC was the predominant failure mode (Fig. 9i) occurring at an average pull-out force of approximatively 28.5 kN, while the other sole competing failure mode was "CC F/A FD" which occurred at the force of approximately 33.5 kN, hence suggesting that the latter failure would be the desired failure mode in E5. Existing studies show that high temperatures can cause the fibre-matrix interface to develop microcracks at the fibre/-polymer interface [58], thereby degrading both the matrix and fibres [59]. Hence, some minor CFRP/adhesive interface failures observed in E5 may have resulted from the developed microcracks at the fibre matrix level. In general, the change of failure mode with time was less pronounced, hence the effects of degradation agents in E5 did not significantly affect the failure mode. This agrees with the pull-out force trend which also was somehow stable with time. Overall, synergic effects between high temperatures and carbonation were the main degradation agents.

Bond strength variation in E6: Marginal variations of the bond strength and a significant decrease in the bond stiffness can be seen from Fig. 11a, b. The almost non-variation of the bond strength with time can be attributed to the improved f_{cc} and f_f that counteracted the loss of f_a and f_{ct}. The CC and the "CC F/A FD" were the only two competing failure modes (Fig. 9i) at an average force of 29 kN and 32.5 kN, respectively. In the former, a very thin layer of concrete detached, which shows that the effects of chlorides on concrete were very minimal, as previously described in Section 3.1. Also, since the exposure of epoxy adhesive to chlorides does not lead to detrimental effect [22], and the f_f is generally immune to chloride exposure [18], the major degradation agents were the interaction of the moisture and carbonation. However, the carbonation played a more role than moisture because of its ability to substantially reduce concrete porosity in the superficial region [31] thereby preventing the rapid ingress of moisture. This is confirmed by the carbonation (C_d) trend (Fig. 7a) that tends to match well with the bond strength trend (Fig. 11a), thereby indicating that the more the C_d the better the bond performance.

Like what is noted in E2, the aggregate bonding to adhesive seemed to control the maximum pull-out force in E6. The more the aggregates were bonded to the adhesive the higher was the pull-out force (Fig. 10.j). This is in line with the findings by [60], where the shape, size and strength of the coarse aggregate played an important role in the pull-off strength.

4. Accelerated ageing *versus* natural ageing

To compare the existing accelerated ageing test (AAT) data with those of natural/outdoor ageing test (NAT) from the present work, a database from different existing studies [24,27–34], was prepared with the following characteristics: i) the database comprised of 99 specimens strengthened with pultruded CFRP laminate strips tested either in a direct or beam single lap shear test configuration, and the environmental conditioning adopted were freeze-thaw cycles, wet-dry cycles, immersion in salt or tap water, moisture, temperature cycles, and splash exposure; ii) the exposure duration was up to 18,000 h (2 years); iii) only epoxy adhesives, and CFRP laminate thickness between 1.0 and 1.4 mm with elastic modulus between 155 and 176 GPa were considered; iv) bond length ranged between 100 and 600 mm, v) concrete compressive strength varied between 25 and 50 MPa.

The bond strength retentions over time for both the above-described database and the data from the present work (denoted as FRPLongDur-E2-E6) are presented in Fig. 12a. It can be observed that the retentions from the existing literature are very scattered ranging between 0.7 and 1.6, while those from the present work lie between 0.9 and 1.2. In fact, after 4 years of exposure, the retentions from NAT data (FRPLongDur-E3-E6) are still generally higher than those from AAT data in the existing literature. On the other hand, assuming 10 % as the maximum allowable non-conservative estimates from all the AAT data in the database, it can be seen from Fig. 12b that the environmental conversion factor (ECF), considering all types of degradation agents, can be suggested to be approximatively 0.75. Furthermore, based on the results from Fig. 12c, the ECF is suggested to be approximately 0.70, 0.75, or 0.90 for structures immersed in water, exposed to freeze-thaw cycles, or elevated temperatures, respectively. This is reasonable because both the bond and its constituent materials are expected to degrade more when exposed to water and freeze-thaws as compared to when exposed to elevated temperatures.

Comparing both the AAT and NAT (Fig. 12d), the ECF for the AAT and NAT is approximately 0.75 and 0.95, respectively, which leads to stating that the exposure of EBR CFRP-to-concrete bond to various outdoor degradation agents for up to 4 years can lead to less degradation as compared to when the bond is exposed to artificially accelerated degradation agents.

5. Conclusion and Recommendations

In this work, the durability of EBR CFRP-concrete bond and its constituent materials was addressed. Specimens were conditioned in 6 different environments. The first two were laboratory-based (i.e., E1 with 20 °C/55 % RH, and E2 with water immersion at 20 °C) and the remaining were outdoor (i.e., E3, E4, E5, and E6 in which the main degradation agents were carbonation, freeze-thaw attacks, elevated temperatures, and airborne chlorides, respectively). The specimens were tested at initial time (T0), and after 1 (T1), 2 (T2), 3 (T3) and 4 (T4)

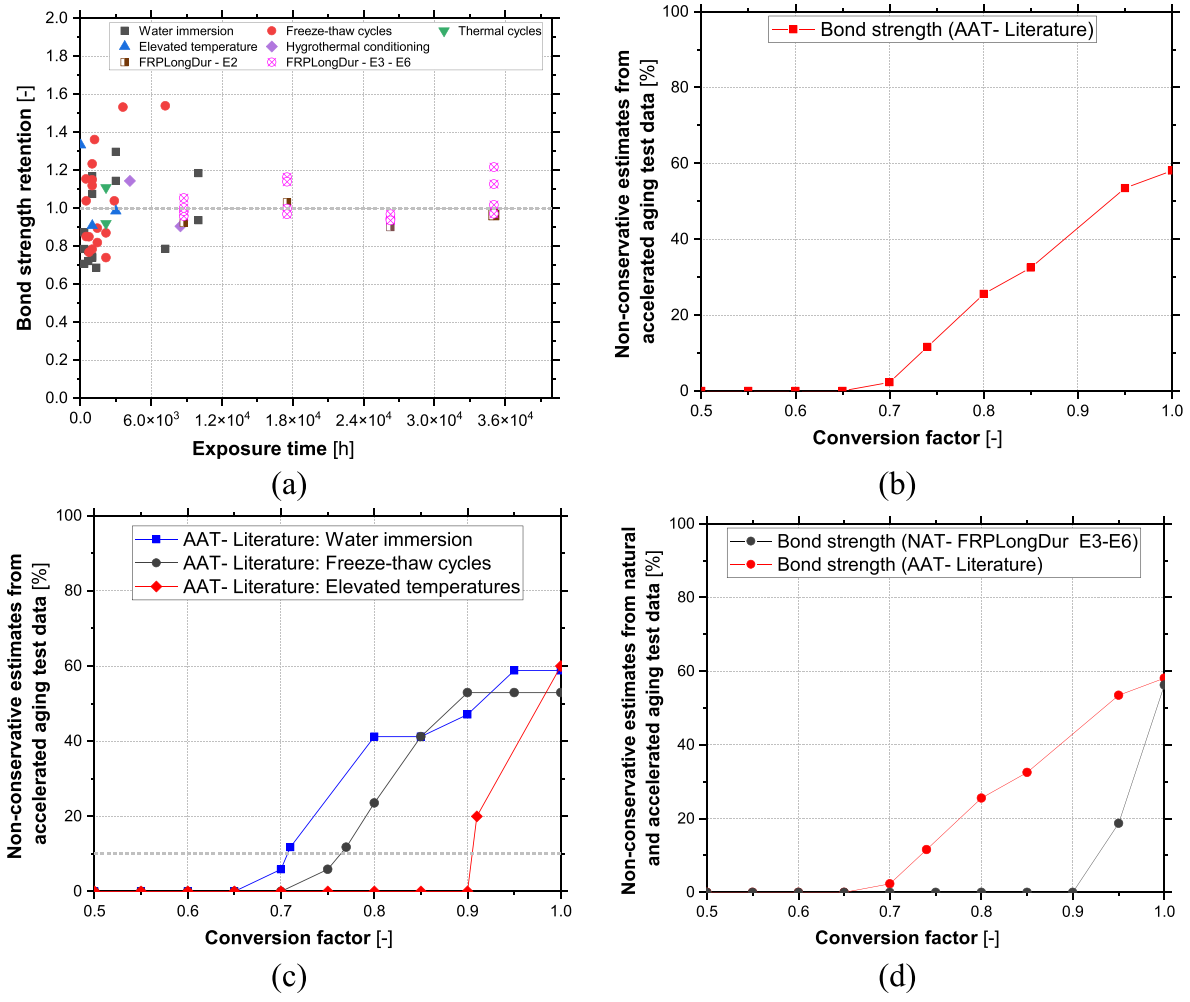

Fig. 12. Natural *vs.* accelerated ageing durability results for EBR technique: (a) bond strength retention from the AAT and NAT data, (b) derivation of the ECF considering all studied degradation agents in AAT data, (c) derivation of the ECF considering a single degradation agent in AAT, (d) comparison of the ECF from the AAT and NAT data.

years of exposure. The key findings are as follows:

- Although the outdoor environments were selected to mainly promote a single degradation agent in each environment, multiple degradation agents occurred; thus, synergistic effects were dominant. That is, carbonation, moisture, and airborne chlorides were the three-competing agents in E6; carbonation and elevated temperature effects were dominant in E3 and E5, and moisture and freeze-thaw effects were dominant in E4.
- *Constituent materials:* Concrete compressive strength (f_{cc}) and elastic modulus (E_c) showed a significant increase in outdoor environments (E3-E6), whereas marginal variations were observed in laboratory environments (E1 and E2). The highest increases were approximately 21 %, 16 %, 21 %, and 17 % in f_{cc}, and 9 %, 12 %, 3 %, and 12 % in E_c for E3, E4, E5, and E6, respectively. Conversely, the concrete pull-off strength (f_{ct}) showed a progressive decrease with time in all the environments studied. On the other hand, the epoxy adhesive generally decreased both its tensile strength (f_a) and tensile elastic modulus (E_a) in all environments, with the lowest values observed in water with reductions of 66.3 % and 75.4 %, respectively. Similarly, the tensile elastic modulus of the CFRP laminate (E_f) also showed a decreasing trend in all environments, the lowest being observed in E6 with a reduction of 13.7 %; however, the CFRP tensile strength (f_f) increased during the first year in all environments because of post-curing, followed by a progressive decrease in the later years. The f_f reduced by 12.3 %, 4.2 %, 6.3 %, 4.7 %, 1.4 %, and 5.6 % and its E_f by 12.6 %, 14.7 %, 10.5 %, 10.5 %, 5.3 %, and 13.7% in E1 to E6, respectively. This showed that E_f degraded faster than f_f.
- *EBR CFRP-to-concrete bond:* Bond strength and bond stiffness varied significantly with time and environment. The latter was found to degrade faster than the former in most of the environments. This was particularly noticeable when the bond was exposed to elevated temperatures (E5), which led to a 39 % reduction in the bond stiffness, whereas there was a marginal change in the bond strength. A tendency for bond strength to decrease over time was generally observed in E1 and E2. In outdoor environments, the bond strength in E3 and E4 showed a tendency to increase with time, but with significant fluctuations that may have resulted from the effects of exposure duration and severity, or from the molecular adjustments in the bonded region resulting from the change in the properties of the constituent materials over time. In contrast, the bond strength was almost unchanged in E5 and E6, indicating that the considered degradation agents did not significantly affect the bond strength in these environments. On the other hand, the bond stiffness showed a progressive-significant decrease in all studied environments. The lowest bond stiffness was observed in E4 with 50% reduction followed by E2 with 40% reduction, and 39% and 35% reductions in E5 and E3, respectively. Smaller reductions were observed in E1 and E6.
- *Failure modes*: Visual examination of the failure modes in EBR showed that the failure mode at the initial time (T0) changed mainly from pure concrete cohesive failure within the concrete alone (or mixed with cohesive failure within the adhesive) to different failures depending on the environmental exposure. Most of the failure modes from different environments were due to interfacial separation between either the adhesive and the concrete substrate or the adhesive and the CFRP. Concrete cohesive failure with a thin concrete layer dominated in E1 and E5; concrete cohesive failure with or without a very thick concrete layer at the free end was predominant in E2; the mixed failure mode of concrete cohesive failure with a thin concrete layer, interfacial adhesive failure at the interface between adhesive and CFRP (at interface regions closest to the adhesive surface or closest to the CFRP laminate surface) dominated in E3 and E4; the mixed failure mode and the concrete cohesive failure with a thin concrete layer were the two competing and predominant failures observed in E6. In general, higher pull-out forces corresponded to specimens with a failure mode that is a mixture of the adhesive-CFRP interaction layer failure and the concrete cohesive failure (than the concrete cohesive failure alone), the larger the area of the former failure the higher the pull-out force. Besides, the fracture/splitting of CFRP always resulted in the highest pull-out force, making it the most desirable failure mode.
- The environmental conversion factor (ECF) for the accelerated ageing test (AAT) based studies is proposed to be 0.75 when all degradation agents are considered as one entity, whereas ECFs of 0.7, 0.75, or 0.90 are proposed to account for the effects of water immersion, freeze-thaws, or high temperature effects, respectively. When comparing both the AAT and natural ageing test (NAT) protocols, ECF values of 0.75 and 0.95 are suggested for the former and latter protocols, respectively, leading to the conclusion that the accelerated ageing test protocols may overestimate the degradation that normally occurs in outdoor environments for 4 years of exposure.

As main recommendation, the authors suggest that studies that attempt to quantify the effects of UV radiations in outdoor environments, in addition to the degradations agents considered in the present work (carbonation, high temperatures, airborne chlorides, and freeze-thaw attacks), can lead to a better understanding on the degradation process of the structures in outdoor environments. Further research comprising both laboratory-based and outdoor environments with comparative perspectives on both environments are highly recommended as they can lead to a better understanding of the durability of the bond between concrete and CFRP laminate.

CRediT authorship contribution statement

Luís Correia: Writing – review & editing, Validation, Supervision, Methodology, Investigation. **Susana Cabral-Fonseca:** Writing – review & editing, Validation, Supervision, Investigation, Data curation. **João Miguel Pereira:** Writing – review & editing, Validation, Formal analysis. **Ricardo Cruz:** Formal analysis, Investigation, Validation, Writing – review & editing. **José Sena-Cruz:** Writing – review & editing, Validation, Supervision, Methodology, Investigation, Funding acquisition, Conceptualization. **Aloys Dushimimana:** Writing – review & editing, Writing – original draft, Investigation, Formal analysis, Conceptualization.

Declaration of Competing Interest

The authors declare that they have no known competing financial interests or personal relationships that could have appeared to influence the work reported in this paper.

Data availability

Data will be made available on request.

Acknowledgements

This work was carried out in the scope of the project FRPLongDur POCI-01-0145-FEDER-016900 (FCT PTDC/ECM-EST/1282/2014) and DURABLE-FRP (PTDC/ECI-EGC/4609/2020) funded by national funds through the Foundation for Science and Technology (FCT) and co-financed by the European Fund of the Regional Development (FEDER) through the Operational Program for Competitiveness and Internationalization (POCI) and the Lisbon Regional Operational Program and, partially financed by the project POCI-01–0145-FEDER-007633 and by FCT/MCTES through national funds (PIDDAC) under the R&D Unit Institute for Sustainability and Innovation in Structural Engineering (ISISE), under reference UIDB/04029/2020 (doi.org/10.54499/UIDB/04029/2020). This work is financed by national funds through FCT under grant agreement [DFA/BD/08403/2021] attributed to the first author. The authors would also like to thank all the companies that have been involved: S&P Clever Reinforcement Iberica Lda., Portuguese Institute for Sea and Atmosphere, I.P. (IPMA, IP), Sika Portugal – Produtos Construção e Indústria, S.A., Hilti Portugal – Produtos e Serviços, Lda., Artecanter – Indústria Criativa, Lda., Tecnipor – Gomes&Taveira Lda.,Vialam – Indústrias Metalúrgicas e Metalomecânicas, Lda., Laboratório Nacional de Engenharia Civil (LNEC, IP), EDP – Energias de Portugal e APDL-SA.

Annex I. : Single-lap shear test results for all the specimens tested from T0 to T4

Time	Specimen	Force (kN)	Slip (mm)	Force (kN)	Slip (mm)	Force (kN)	Slip (mm)
T0	No.1	34.06	0.65	-	-	-	-
	No.2	25.47	0.43	-	-	-	-
	No.3	33.62	0.55	-	-	-	-
	No.4	28.92	0.50	-	-	-	-
		E1		**E2**		**E3**	
T1	No.1	34.18	0.31	31.55	0.30	34.17	0.25
	No.2	26.3	0.20	27.74	0.23	31.06	0.28
	No.3	33.69	0.45	29.53	0.27	33.24	0.62
	No.4	26.77	0.49	28.09	0.24	29.58	0.26
T2	No.1	31.13	0.37	32.43	0.28	36.43	0.59
	No.2	26.36	0.21	30.37	0.23	32.82	0.33
	No.3	31.58	0.41	35.40	0.23	38.32	0.39
	No.4	26.32	0.22	28.63	0.30	35.87	0.27
T3	No.1	25.43	0.40	31.28	0.18	29.49	0.45
	No.2	24.02	0.40	27.45	0.10	29.86	0.38
	No.3	31.31	0.47	28.65	0.06	30.90	0.51
	No.4	24.84	0.45	24.57	0.09	28.41	0.48
T4	No.1	35.27	0.67	27.91	0.18	36.80	0.72
	No.2	28.97	0.58	35.51	0.52	30.93	0.60
	No.3	28.44	0.58	34.22	0.38	38.06	0.27
	No.4	24.47	0.58	35.67	0.57	-	-
		E4		**E5**		**E6**	
T1	No.1	28.81	0.18	33.52	0.52	37.04	0.42
	No.2	31.87	0.12	26.82	0.23	26.74	0.28
	No.3	28.35	0.29	34.21	0.24	31.89	0.32
	No.4	30.89	0.16	27.88	0.17	28.39	0.34
T2	No.1	32.79	0.27	34.92	0.27	29.72	0.35
	No.2	39.81	0.28	29.52	0.32	34.56	0.25
	No.3	30.83	0.33	29.18	0.24	30.32	0.25
	No.4	36.11	0.28	29.61	0.52	27.19	0.22
T3	No.1	31.49	0.27	27.65	0.39	34.59	0.35
	No.2	31.20	0.26	33.46	0.37	28.15	0.29
	No.3	29.09	0.26	29.08	0.23	25.56	0.29
	No.4	29.63	0.40	31.45	0.45	33.83	0.56
T4	No.1	37.27	0.74	28.4	0.29	32.90	0.31
	No.2	36.68	0.35	34.65	0.40	33.55	0.31
	No.3	40.27	0.63	30.87	0.46	29.93	0.28
	No.4	37.21	0.37	27.38	0.33	32.74	0.21

E1-E6: studied environments, T1-T4: exposure periods (in years)

Annex II: Single-lap shear test results: Pull-out force vs. loaded end slip curves for all specimens tested up to 4 years

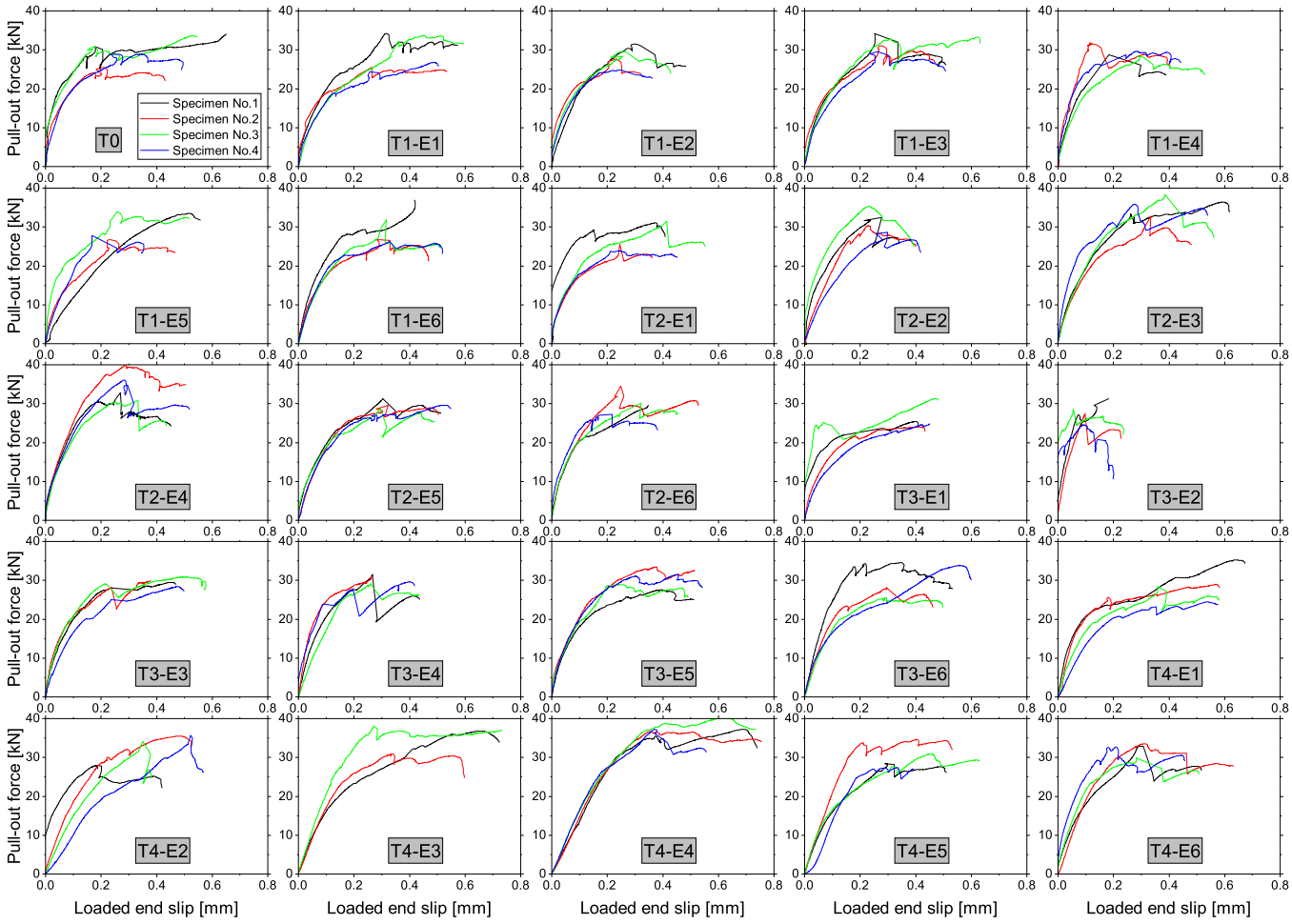

References

[1] F. Hermansson, S. Heimersson, M. Janssen, M. Svanström, Can carbon fiber composites have a lower environmental impact than fiberglass? Resour. Conserv. Recycl. 181 (2022) https://doi.org/10.1016/j.resconrec.2022.106234.

[2] S. Maiti, M.R. Islam, M.A. Uddin, S. Afroj, S.J. Eichhorn, N. Karim, Sustainable fiber-reinforced composites: a review, Adv. Sustain. Syst. 6 (2022), https://doi.org/10.1002/adsu.202200258.

[3] I.S. Abbood, S.A. Odaa, K.F. Hasan, M.A. Jasim, Properties evaluation of fiber reinforced polymers and their constituent materials used in structures - a review, Mater. Today Proc. 43 (2021) 1003–1008, https://doi.org/10.1016/j.matpr.2020.07.636.

[4] H.H. Mhanna, R.A. Hawileh, J.A. Abdalla, Shear strengthening of reinforced concrete beams using CFRP wraps, Procedia Struct. Integr. 17 (2019) 214–221, https://doi.org/10.1016/j.prostr.2019.08.029.

[5] L. Correia, T. Teixeira, J. Michels, J.A.P.P. Almeida, J. Sena-Cruz, Flexural behaviour of RC slabs strengthened with prestressed CFRP strips using different anchorage systems, Compos. Part B Eng. 81 (2015) 158–170, https://doi.org/10.1016/j.compositesb.2015.07.011.

[6] CEB-FIP, fib90 Bulletin:Externally Applied FRP reinforcement for Concrete structures, 2019.

[7] J.S. Cruz, J. Barros, Modeling of bond between near-surface mounted CFRP laminate strips and concrete, Comput. Struct. 82 (2004) 1513–1521, https://doi.org/10.1016/j.compstruc.2004.03.047.

[8] N.M. Huang, J.J. Chang, M.T. Liang, Effect of plastering on the carbonation of a 35-year-old reinforced concrete building, Constr. Build. Mater. 29 (2012) 206–214, https://doi.org/10.1016/j.conbuildmat.2011.08.049.

[9] V. Talakokula, S. Bhalla, R.J. Ball, C.R. Bowen, G.L. Pesce, R. Kurchania, B. Bhattacharjee, A. Gupta, K. Paine, Diagnosis of carbonation induced corrosion initiation and progression in reinforced concrete structures using piezo-impedance transducers, Sens. Actuators, A Phys. 242 (2016) 79–91, https://doi.org/10.1016/j.sna.2016.02.033.

[10] X. han Shen, Q. feng Liu, Z. Hu, W. qiang Jiang, X. Lin, D. Hou, P. Hao, Combine ingress of chloride and carbonation in marine-exposed concrete under unsaturated environment: A numerical study, Ocean Eng. 189 (2019) 106350, https://doi.org/10.1016/j.oceaneng.2019.106350.

[11] S.K. Roy, D.O. Northwood, K.B. Pohs, Effect of plastering on the carbonation of a 19-year-old reinforced concrete building, Constr. Build. Mater. 29 (2012) 206–214, https://doi.org/10.1016/j.conbuildmat.2011.08.049.

[12] A.F.Al Fuhaid, A. Niaz, Carbonation and Corrosion Problems in Reinforced Concrete Structures, Buildings 12 (2022) 1–20, https://doi.org/10.3390/buildings12050586.

[13] J. Zhao, G. Cai, L. Cui, A. Si Larbi, K.D. Tsavdaridis, Deterioration of basic properties of the materials in FRP-strengthening RC structures under ultraviolet exposure, Polymers 9 (2017), https://doi.org/10.3390/polym9090402.

[14] Z. Mi, Y. Hu, Q. Li, Z. An, Effect of curing humidity on the fracture properties of concrete, Constr. Build. Mater. 169 (2018) 403–413, https://doi.org/10.1016/j.conbuildmat.2018.03.025.

[15] Y. Wang, S. Nanukuttan, Y. Bai, P.A.M. Basheer, Influence of combined carbonation and chloride ingress regimes on rate of ingress and redistribution of chlorides in concretes, Constr. Build. Mater. 140 (2017) 173–183, https://doi.org/10.1016/j.conbuildmat.2017.02.121.

[16] H. Kuosa, R.M. Ferreira, E. Holt, M. Leivo, E. Vesikari, Effect of coupled deterioration by freeze-thaw, carbonation and chlorides on concrete service life, Cem. Concr. Compos. 47 (2014) 32–40, https://doi.org/10.1016/j.cemconcomp.2013.10.008.

[17] P. Fernandes, P. Silva, L. Correia, J. Sena-cruz, Durability of an epoxy adhesive and a CFRP laminate under different exposure conditions, in: Third Conf. Smart Monit. Assess. Rehabil. Civ. Struct. 2015, 2015: p. 9.

[18] R. Cruz, L. Correia, A. Dushimimana, S. Cabral-Fonseca, J. Sena-Cruz, Durability of epoxy adhesives and carbon fibre reinforced polymer laminates used in strengthening systems: Accelerated ageing versus natural ageing, Materials 14 (2021), https://doi.org/10.3390/ma14061533.

[19] S. Cabral-fonseca, J.R. Correia, J. Custódio, H.M. Silva, A.M. Machado, J. Sousa, Durability of FRP - concrete bonded joints in structural rehabilitation: a review,

Int. J. Adhes. Adhes. 83 (2018) 153–167, https://doi.org/10.1016/j.ijadhadh.2018.02.014.
[20] S.A. Grammatikos, R.G. Jones, M. Evernden, J.R. Correia, Thermal cycling effects on the durability of a pultruded GFRP material for off-shore civil engineering structures, Compos. Struct. 153 (2016) 297–310, https://doi.org/10.1016/j.compstruct.2016.05.085.
[21] E. Cui, S. Jiang, J. Wang, X. Zeng, Bond behavior of CFRP-concrete bonding interface considering degradation of epoxy primer under wet-dry cycles, Constr. Build. Mater. 292 (2021) 123286, https://doi.org/10.1016/j.conbuildmat.2021.123286.
[22] P. Silva, P. Fernandes, J. Sena-Cruz, J. Xavier, F. Castro, D. Soares, V. Carneiro, Effects of different environmental conditions on the mechanical characteristics of a structural epoxy, Compos. Part B Eng. 88 (2016) 55–63, https://doi.org/10.1016/j.compositesb.2015.10.036.
[23] D. dong Hu, J. xun Lyu, T. Liu, M. dong Lang, L. Zhao, Solvation effect of CO2 on accelerating the curing reaction process of epoxy resin, Chem. Eng. Process. - Process. Intensif. 127 (2018) 159–167, https://doi.org/10.1016/j.cep.2018.01.027.
[24] S. Liu, Y. Pan, H. Li, G. Xian, Durability of the bond between CFRP and concrete exposed to thermal cycles, Mater. (Basel) 12 (2019), https://doi.org/10.3390/ma12030515.
[25] F. Jiang, X. Han, Y. Wang, P. Wang, T. Zhao, K. Zhang, Effect of freeze-thaw cycles on tensile properties of CFRP, bond behavior of CFRP-concrete, and flexural performance of CFRP-strengthened concrete beams, Cold Reg. Sci. Technol. 194 (2022) 103461, https://doi.org/10.1016/j.coldregions.2021.103461.
[26] C. Helbling, V. Karbhari, Durability of composites in aqueous environments, in: Durab. Compos. Civ. Struct. Appl., Elsevier, Amsterdam, The Netherlands, 2007: pp. 31–71.
[27] M.F. Green, L.A. Bisby, Y. Beaudoin, P. Labossière, Effect of freeze-thaw cycles on the bond durability between fibre reinforced polymer plate reinforcement and concrete, Can. J. Civ. Eng. 27 (2000) 949–959, https://doi.org/10.1139/l00-031.
[28] M. Leone, S. Matthys, M.A. Aiello, Effect of elevated service temperature on bond between FRP EBR systems and concrete, Compos. Part B Eng. 40 (2009) 85–93, https://doi.org/10.1016/j.compositesb.2008.06.004.
[29] P. Colombi, G. Fava, C. Poggi, Bond strength of CFRP-concrete elements under freeze-thaw cycles, Compos. Struct. 92 (2010) 973–983, https://doi.org/10.1016/j.compstruct.2009.09.044.
[30] J.R. Cromwell, K.A. Harries, B.M. Shahrooz, Environmental durability of externally bonded FRP materials intended for repair of concrete structures, Constr. Build. Mater. 25 (2011) 2528–2539, https://doi.org/10.1016/j.conbuildmat.2010.11.096.
[31] K. Benzarti, S. Chataigner, M. Quiertant, C. Marty, C. Aubagnac, Accelerated ageing behaviour of the adhesive bond between concrete specimens and CFRP overlays, Constr. Build. Mater. 25 (2011) 523–538, https://doi.org/10.1016/j.conbuildmat.2010.08.003.
[32] F. Al-Mahmoud, J.M. Mechling, M. Shaban, Bond strength of different strengthening systems - concrete elements under freeze-thaw cycles and salt water immersion exposure, Constr. Build. Mater. 70 (2014) 399–409, https://doi.org/10.1016/j.conbuildmat.2014.07.039.
[33] Y. Pan, G. Xian, M.A.G. Silva, Effects of water immersion on the bond behavior between CFRP plates and concrete substrate, Constr. Build. Mater. 101 (2015) 326–337, https://doi.org/10.1016/j.conbuildmat.2015.10.129.
[34] Y. Pan, G. Xian, H. Li, Effects of Freeze-Thaw Cycles on the Behavior of the Bond between CFRP Plates and Concrete Substrates, J. Compos. Constr. 22 (2018) 1–14, https://doi.org/10.1061/(asce)cc.1943-5614.0000846.
[35] R. Cruz, L. Correia, S. Cabral-Fonseca, J. Sena-Cruz, Durability of bond between NSM CFRP strips and concrete under real-time field and laboratory accelerated conditioning, J. Compos. Constr. 26 (2022) 1–15, https://doi.org/10.1061/(asce)cc.1943-5614.0001262.
[36] IPQ, IPQ (Instituto Português da Qualidade). 2013. NP EN 12390-13. Testing Hardened Concrete. Part 13: Determination of Secant Modulus of Elasticity in Compression, Instituto Português da Qualidade (IPQ)., Caparica, Portugal, 2013.
[37] IPQ, 2011. NP EN 12390-3. Testing Hardened Concrete. Part 3: Compressive Strength of Test Specimen, Instituto Português da Qualidade (IPQ), Caparica, Portugal, 2011.
[38] BSI, BSI (British Standards Institution). Products and systems for the pro- tection and repair ofconcrete structures – Test methods – Measurement ofbond strength by pull-off. EN 1542., London: BSI, 1999.
[39] ISO, ISO 527-2:2012—Plastics—Determination of tensile properties—Part 2: Test conditions for moulding and extrusion plastics, Genève, Switzerland, 2012.
[40] ISO, ISO 527-5:2009 Part 5: Test Conditions for Unidirectional Fibre-Reinforced Plastic composites. Plastic—Determ. Tensile Prop., Inte Genève, Switzerland, 2009; Volume 1, 2009.
[41] CNR-DT 200 R1, Guide for the design and construction of externally bonded frp systems for strengthening existing structures; CNR-DT 200 R1/2013;, Rome, Italy, 2013.
[42] T.P. Hills, F. Gordon, N.H. Florin, P.S. Fennell, Statistical analysis of the carbonation rate of concrete, Cem. Concr. Res. 72 (2015) 98–107, https://doi.org/10.1016/j.cemconres.2015.02.007.
[43] N. Bouzoubaâ, A. Bilodeau, B. Tamtsia, S. Foo, Carbonation of fly ash concrete: laboratory and field data, Can. J. Civ. Eng. 37 (2010) 1535–1549, https://doi.org/10.1139/L10-081.
[44] L. Jiang, Y. Zhang, Anal. Calc. Length half – Carbonate zone Concr. [Chin.], Ind. Constr. 29 (1999) 4–8.
[45] H. Tseng, J. Hsia, Concrete carbonation and durability prediction[in Chinese], Hunan Commun, Sci. Technol. 32 (2006) 121–126.
[46] A. Dushimimana, A.A. Niyonsenga, F. Nzamurambaho, A review on strength development of high performance concrete, Constr. Build. Mater. 307 (2021) 124865, https://doi.org/10.1016/j.conbuildmat.2021.124865.
[47] S.N. Shoukry, G.W. William, B. Downie, M.Y. Riad, Effect of moisture and temperature on the mechanical properties of concrete, Constr. Build. Mater. 25 (2011) 688–696, https://doi.org/10.1016/j.conbuildmat.2010.07.020.
[48] H. Peng, Y. Liu, C.S. Cai, J. Yu, J. Zhang, Experimental Investigation of Bond between Near-Surface-Mounted CFRP Strips and Concrete under Freeze-Thawing Cycling, J. Aerosp. Eng. 32 (1) (2019) 10, https://doi.org/10.1061/(asce)as.1943-5525.0000937.
[49] M.I. Kabir, R. Shrestha, B. Samali, Effects of applied environmental conditions on the pull-out strengths of CFRP-concrete bond, Constr. Build. Mater. 114 (2016) 817–830, https://doi.org/10.1016/j.conbuildmat.2016.03.195.
[50] M. Massou, N. Babu, G. Xian, Experimental study on the mechanical properties of CFRP/epoxy composite plates under seawater immersion, Structures 54 (2023) 48–57, https://doi.org/10.1016/j.istruc.2023.05.042.
[51] D. Mostofinejad, M. Mohammadi, Effect of freeze–thaw cycles on FRP-concrete bond strength in EBR and EBROG Systems, J. Compos. Constr. 24 (2020) 1–12, https://doi.org/10.1061/(asce)cc.1943-5614.0001010.
[52] L. Hong, R.M. Duo, S.Y. Wang, L.X. Li, Influence of freeze-thaw cycles on bonded interface performance between CFRP and high strength concrete, Appl. Mech. Mater. 638–640 (2014) 1516–1520, https://doi.org/10.4028/www.scientific.net/AMM.638-640.1516.
[53] R.M. Faysal, M.M.H. Bhuiyan, K.Al Momin, T. Tafsirojjaman, Y. Liu, A review on the advances of the study on FRP-Concrete bond under hygrothermal exposure, Constr. Build. Mater. 363 (2023) 129818, https://doi.org/10.1016/j.conbuildmat.2022.129818.
[54] M. Savvilotidou, A.P. Vassilopoulos, T. Keller, Durability and Fatigue Performance of Cold-Curing Structural Adhesives in Bridge Construction, École Polytechnique Fédérale de Lausanne (EPFL), 2017. https://infoscience.epfl.ch/record/230442?ln=en.
[55] J. Tatar, S. Milev, Durability of externally bonded fiber-reinforced polymer composites in concrete structures: a critical review, Polymers 13 (2021) 1–26, https://doi.org/10.3390/polym13050765.
[56] J. Lee, J. Kim, C.E. Bakis, T.E. Boothby, Durability assessment of FRP-concrete bond after sustained load for up to thirteen years, Compos. Part B Eng. 224 (2021) 109180, https://doi.org/10.1016/j.compositesb.2021.109180.
[57] A.K. Al-Tamimi, R.A. Hawileh, J.A. Abdalla, H.A. Rasheed, R. Al-Mahaidi, Durability of the bond between CFRP plates and concrete exposed to harsh environments, J. Mater. Civ. Eng. 27 (2015) 04014252, https://doi.org/10.1061/(asce)mt.1943-5533.0001226.
[58] L.T. Drzal, M.J. Rich, M.F. Koenig, P.F. Lloyd, Adhesion of graphite fibers to epoxy matrices: ii. the effect of fiber finish, J. Adhes. 16 (1983) 133–152, https://doi.org/10.1080/00218468308074911.
[59] C. Bockenheimer, D. Fata, W. Possart, New aspects of aging in epoxy networks. I. Thermal aging, J. Appl. Polym. Sci. 91 (2004) 361–368, https://doi.org/10.1002/app.13092.
[60] E. Bonaldo, J.A.O. Barros, P.B. Lourenço, Bond characterization between concrete substrate and repairing SFRC using pull-off testing, Int. J. Adhes. Adhes. 25 (2005) 463–474, https://doi.org/10.1016/j.ijadhadh.2005.01.002.